Lignin-containing cellulose nanofibrils (LCNF): processing and characterization

by

María Celeste Iglesias

A thesis submitted to the Graduate Faculty of
Auburn University
in partial fulfillment of the
requirements for the Degree of
Master of Science

Auburn, Alabama
August 4, 2018

Key words:

lignin-containing cellulose nanofibrils, LCNF, rheology, residual lignin

Approved by

Dr. María Soledad Peresin, Professor of Forestry and Wildlife Science
Dr. Brian Via, Professor of Forestry and Wildlife Science
Dr. María Lujan Auad, Professor of Chemical Engineer
Dr. Thomas Elder, Research Scientist, USDA-Forest Service
Dr. Zhihua Jiang, Professor of Chemical Engineer

Abstract

Currently, the global dependence on oil as a source of energy and raw materials has dramatically increased, creating practical and environmental concerns. This has led to several efforts towards replacing this non-renewable with environmentally friendly alternatives. In this sense, lignocellulosic materials have gained attention over the years as an alternative for the replacement of oil-based products due to their abundancy and renewability. Such lignocellulosic materials can be found in nature as a combination of polysaccharides, such as cellulose and hemicelluloses –the structural components of biomass-, embedded in lignin, which act as an adhesive for the structure.

Renewable, biodegradable and biocompatible lignocellulosic materials with nano-scale dimensions are known as nanocellulose. The methods applied to obtain nanocellulose usually involve chemical-, mechanical-, and enzymatic treatments, or a combination of thereof, giving rise to different types of nanocellulose. Most commonly, the term nanocellulose refers to cellulose nanocrystals (CNC) and cellulose nanofibrils (CNF), the latter being the object of the present study. Both types of nanocellulose can be utilized in novel applications such as packaging, functional nanocomposites, emulsion stabilizers and in the pharmaceutical and medical fields, due to their unique properties such as high aspect ratio, high strength, low density, and high capacity for chemical–modification.

The chemical composition and properties of the starting lignocellulosic material utilized for CNF production will play an important role in the behavior of the resulting materials after fibrillation, as the individual components interact at a very fundamental level.

The main source for CNF is bleached cellulose pulp, where lignin and non-cellulosic polysaccharides have been removed by chemical treatments. During the pulping processes the fibers undergo chemical reactions that will affect their surface properties, which are the main factors responsible for their interactions with the medium in which they will be dispersed. Understanding the final properties of cellulose fibers after the pulping processes, in terms of functional groups and composition, allows a deeper understanding of the final CNF properties such as morphology, thermal stability, and chemical composition.

Although, the removal of the cell wall components has been widely used, the presence of residual lignin in raw materials for the production of lignin containing cellulose nanofibrils (LCNF) might be beneficial as demonstrated by the reduction of dewatering time and oxygen permeability of films. Additionally, the utilization of unbleached cellulose pulp to produce LCNF results in higher yields while reducing costs, due to the lower energy consumption during the manufacture process. Furthermore, from an environmental point of view, the production of LCNF could be beneficial since the processes of lignin removal as well as the following bleaching steps are no longer necessary.

The main objective of this work is to study how the remaining lignin on the starting cellulose fibers, affect the properties of the resulting CNFs, allowing for a better utilization of LCNF and selection of final applications. Different characterization techniques were utilized to assess the relationship between the lignin content and the characteristics of the nanofibrils. Morphology of the CNF was studied using optical microscopy, scanning electron microscopy (SEM), and atomic force microscopy (AFM). Fibril diameter and diameter distributions for CNF with different levels of residual lignin were investigated based on AFM images. Fourier-transform infrared spectroscopy (FTIR), thermogravimetric analysis (TGA), and X-ray powder diffraction (XRD) were used to analyze chemical composition, thermal decomposition, and degree of

crystallinity, respectively. The stability of the colloidal suspensions was assessed by zeta-potential and charge density analyses. Finally, rheological behavior of the samples was evaluated and correlated with all the above mentioned properties of LCNF.

Acknowledgements

First, I would like to thank my mentor and advisor, Dr. Maria Soledad Peresin. Thank you for trusting in me, for offering me this invaluable opportunity, and for teaching and helping me not only in my academic but also personal development. Thank you for encouraging me every day. Thank you to my committee members, Dr. Maria Lujan Auad, Dr. Brian Via, Dr. Thomas Elder, and Dr. Zhihua Jiang, for sharing your knowledge and experience. I want to especially thank to Dr. Beatriz Vega, having you in our group made us grow, I really appreciate all the time you spent to help and teach me, thank you for your infinite patience

I also would like to thank Dr. Charles Frazier, Dr. Ann Norris, and Niloofar Yousefi-Shivyari from Virginia Tech, for the collaboration with the rheological analyses. To Dr. Karin Stana and her group at University of Maribor, Slovenia, for their hospitality and support during my time there.

To Raquel Martin Sampedro from INIA, Spain, for the cellulose pulps and for her time and valuable help; to Panu Lathinen from VTT, Finland, for preparing the nanocellulose samples used in this work, and to Mikkelson Atte also from VTT, for the molecular weight measurements.

Huge and special thanks to all the faculty members, staff, colleagues, and friends at the Forest Products Development Center, thank you for sharing with me your knowledge and valuable opinions, but principally for your friendship during all this time, which made this experience more gratifying.

Thank you to my Auburn family: Marina, Simon, Nati, Fer, Diego, Caren, Laura, without any doubt you are a fundamental piece in this achievement. Having you during this time made this experience irreplaceable.

Finally, I want to thank and dedicate this thesis to my dear parents Luis and Vivi, for your constant love and support to fulfill my goals; to my siblings Flori and Lu; to my niece, my little love Justina, and finally to him, Pablo, there are not enough words, just thank you for following me and supporting me all over the world, for your constant patience, generosity and love. For all of you is this thesis, because being far from you will be always the most difficult chapter.

Table of content

Abstract ii

Acknowledgements v

List of tables xi

List of figures xii

Appendix: List of publications xiv

Chapter 1 1

1.1. Introduction 1

1.2. Wood as raw material 3

1.3. Constituents of wood 4

1.3.1. Cellulose 5

1.3.2. Hemicellulose 10

1.3.3. Lignin 11

1.4. Pulping methods 12

1.4.1. Kraft pulping 14

1.4.2. Sulfite pulping 15

1.5. Effects of pulping on surface properties of cellulose fibers 16

1.5.1. Crystallinity..... 16

1.5.2. Surface functionalized groups..... 17

1.5.3. Chromophores groups..... 18

1.5.4. Lignin-carbohydrates complexes (LCC)..... 19

1.5.5. General properties..... 19

1.6. Bleaching process 20

1.7. Surface properties after bleaching 21

1.8. Nanocellulose..... 22

1.8.1. Cellulose nanofibrils (CNF)..... 23

1.9. Conclusions..... 25

References..... 27

Chapter 2..... 39

2.1. Introduction..... 39

2.2. Optimization CNF production with Masuko Supermasscolloider..... 43

2.3. Materials and methods..... 45

2.3.1. Raw material 45

2.3.2. Characterization of the raw material for LCNF production..... 47

2.3.3. LCNF Production 47

2.3.4. Self-standing LCNF films 48

2.3.5. Characterization of LCNF suspensions 48

2.3.5.1. Zeta-potential 48

2.3.5.2. Average molar mass measurement 48

2.3.5.3. Thermogravimetric Analysis (TGA) 49

2.3.5.4. Fourier-transform infrared spectroscopy with attenuated total reflectance accessory (ATR-FTIR) 49

2.3.5.5. X-ray powder diffraction (XRD) 49

2.3.5.6. Microscopy 50

2.3.5.7. Rheological behavior 51

2.3.5.8. Surface contact angle measurements (SCA) 52

2.4. Results and discussion 53

2.4.1. Wood characterization of the raw material for LCNF production 53

2.4.2. Self-standing films 54

2.4.3. Characterization of LCNF suspensions 55

2.4.3.1.Zeta-potential 55

2.4.3.2. Molecular Weight Analysis 56

2.4.3.3. Thermogravimetric Analysis (TGA) 57

2.4.3.4. Fourier-transform infrared spectroscopy with attenuated total reflectance accessory (ATR-FTIR) 59

2.4.3.5. X-ray powder diffraction (XRD) 61

2.4.3.6. Microscopy 62

2.4.3.7. Rheological measurements 67

2.4.3.8. Surface contact angle measurements (SCA) 72

2.5. Conclusions 73

2.6. Future work 74

2.6.1. Use of LCNF as additive in drilling fluids 74

2.6.2. Characterization techniques 75

References 76

List of tables

Table 1.1.	Wood chemistry composition in percentage of dry wood weight	4
Table 2.1.	Cooking conditions of the cellulose pulps used to produce LCNF	46
Table 2.2.	Wood chips and cellulose pulps quantification results expressed as percentage of analyzed sample	53
Table 2.3.	Characterization results of LCNF	55
Table 2.4.	Results from size exclusion chromatography for LCNF	56
Table 2.5.	Power-law parameters and regression values (R^2) fitted to the data ($\eta = K\dot{\gamma}^{n-1}$)	70
Table 2.6.	SCA average results and standard deviations	73

List of figures

Figure 1.1.	Wood components arrangement on the cell wall layers. Reprinted from (Wang and Luo 2017) with permission from De Gruyter.	5
Figure 1.2.	Cellulose chain structure. Reprinted from (Kontturi et al. 2006) with permission from Royal Society of Chemistry.	6
Figure 1.3.	Intra and inter-molecular interactions within and between cellulose chains. Adapted from (Kontturi et al. 2003) with permission from Royal Society of Chemistry.	7
Figure 1.4.	Hydrogen bonding patterns for Iα and Iβ. Adapted from (Moon et al. 2011) with permission from Royal Society of Chemistry.	8
Figure 1.5.	Polymorphs of cellulose and their obtaining sequence. Reprinted from (Lavoine et al. 2012) with permission from Elsevier.	9
Figure 1.6.	Three lignin precursors. Reprinted from (Chakar and Ragauskas 2004) with permission from Elsevier.	12
Figure 1.7.	Estimated total capacity US pulp production (2020). Information adapted from (FAO 2016).	14
Figure 2.1.	Masuko Supermasscolloider (MKZA10-15J) acquired by Dr. Maria Soledad Peresin.	44
Figure 2.2.	Rheological measurements of LCNF samples; a) load, b) oil barrier, and c) after measurement sample containing 10.2% lignin remained attach to the upper plate.	52

Figure 2.3.	LCNF self-standing films made by solvent casting, a) 0.6, b) 1.7, c) 4.7, and d) 10.2 % of lignin.	54
Figure 2.4.	Thermal stability of LCNF samples containing; a) 0.6, b) 1.7, c) 4.7, and d) 10.2% lignin	57
Figure 2.5.	Derivative weight for LCNF containing; a) 0.6, b) 1.7, c) 4.7, and d) 10.2% lignin	58
Figure 2.6.	FT-IR spectra of the LCNF containing a) 0.6, b) 1.7, c) 4.7, and d) 10.2 % of lignin.	61
Figure 2.7.	XRD spectra of LCNF samples.	62
Figure 2.8.	Optical microscopies of LCNF containing a) 0.6, b) 1.7, c) 4.7, and d) 10.2 % of lignin.	63
Figure 2.9.	Scanning Electron Microscopies (SEM) of LCNF containing a) 0.6, b) 59 1.7, c) 4.7, and d) 10.2 % of lignin.	64
Figure 2.10.	Atomic Force Microscopies (AFM) of LCNF containing a) 0.6, b) 1.7, 60 c) 4.7, and d) 10.2 % of lignin.	65
Figure 2.11.	Diameters distribution for LCNF samples containing; 1) 0.6, 2) 1.7, 3) 4.7, and 4) 10.2% of lignin.	66
Figure 2.12.	Steady state flow curves for LCNF a) UP curves, and b) DOWN curves.	68
Figure 2.13.	Up and down flow curves for L-CNF a) 0.6% lignin, b) 1.7% lignin, c) 4.7% lignin, and d) 10.2 % lignin.	69
Figure 2.14.	Oscillation curves for LCNF samples with an applied stress of 5 Pa. G' (bold), G'' (empty) for 0.6% lignin (▲, Δ), 1.7% lignin (●, ○), 4.7% lignin (■, □), and 10.2% lignin (♦, ◊).	71
Figure 2.15.	Rheological behavior of a LCNF containing 10.2 % at pH = 5 (● and ○), and pH = 7 (■ and □).	72

Appendix: List of publications

Paper I: Iglesias M. C. et al. (2018) (In preparation), A comprehensive review on the effects of pulping and bleaching processes on the surface chemistry of cellulose fibers for nanocellulose production.

Paper II: Iglesias M. C. et al. (2018). (In preparation), Effects of residual lignin on the rheological properties of lignin containing cellulose nanofibrils (LCNF) suspensions.

Contributions not included in this dissertation

Paper III: Abbati de Assis, C., **Iglesias, M.C.**, Bilodeau, M., Johnson, D., Phillips, R., Peresin, M.S., Bilek, E.M., Rojas, O.J, Venditti, R., Gonzalez, R. (**2017**). Cellulose microand nanofibrils (CMNF) manufacturing-financial and risk assessment. *Biofuels, Bioproducts and Biorefining*. **DOI: 10.1002/bbb.1835**.

Paper IV: Villada Y., **Iglesias M. C.**, Casis N., Peresin M. S., Erdmann E., and Estenoz D. (**Submitted**: *Cellulose*). Cellulose nanofibrils as a replacement additive of xanthan gum (XGD) in water based muds (WBMs) for a shale formation.

Paper V: Solala I., **Iglesias M. C**., and Peresin M. S. (to be **submitted to Green Chemistry August 2018**). Perspectives on lignin-containing cellulose nanofibrils (LCNF): a review.

Chapter 1

Literature review: Pulping processes and their effects on cellulose fibers and impact on nanofibrillated cellulose properties

1.1. Introduction

Cellulose is an abundant and natural material which has been used for centuries to supply human necessities and as the primary source for the production of pulp and paper (Klemm et al. 2005; Dufresne 2017). It was about 105 AC in China, when the first paper was developed; at that time, cellulose properties were taken into consideration even without being completely aware of it (Sixta 2006). At that time, the paper manufacturing process was based on the hydration of plant tissues in water, followed by cutting and pressing the material. By doing this, a thin network of cellulose fibers was formed onto the fabric leading to the production of the first paper sheet. Over the years, the production of pulps and papers has evolved until the modern-day technologies; in addition, a variety of plants are now being used, as more sophisticated and complex industries have been initiated. With this, not only cutting down the raw material, but also carrying out chemical treatments, has made the cellulose industry a wide and profitable business. With a broad spectrum of final products, this industry is now able to produce more specialized merchandise, from thick boards to very thin and soft skin care tissues, as well as cellulose pulps with diverse chemical compositions and properties.

During the last century, there was enormous growth and industrialization of societies, and the utilization of petroleum-based materials started to predominate. These changes resulted in a dependence on oil for energy and materials, concern for the availability of such resources in the long term, and consequent calls for their replacement with renewable and more environmentally friendly alternative resources. The amount of biomass globally available at relatively low cost makes it an appealing option for the replacement of materials, chemicals and energy that are currently derived from fossil sources.

As mentioned before, cellulose –in particular from wood sources- is one of the most abundant natural and renewable resources on the planet. Although the current utilization of cellulose is to produce the most common commodities, such as paper, board, and tissue. With the decline of the paper consumption and digitization of information, the pulp and paper industry has been actively seeking new alternative processes and products from cellulose with improved properties, with extensive efforts by the academic and industrial sectors, to develop value-added and high-performance products (Xu et al. 2013; Li et al. 2015).

With the emergence of nanotechnology, the possibility of applications at this scale has been a research topic of increased importance for different proposed uses (Moon et al. 2006). Nanotechnology is concerned with the ability to manipulation of materials at scales of 100 nm or lower (Kamel 2007); and with all these materials, properties of the most fundamental levels show behavior that is distinctly different from those in the bulk (Kamel 2007). Following this trend, cellulose shows remarkable improvements in its mechanical and surface properties at the nanoscale, properties that can be advantageous for a wide variety of applications.

At a very fundamental level, intermolecular interactions play a very important role in the properties of cellulose since they are the main drivers for the material behavior and final properties.

Surface properties dictate the interactions that materials will have towards the medium in which they are placed and with other components (Ratner et al. 2013).

The aim of this work is to provide an overview of how the different modifications that occur during the kraft and sulfite pulping processes will affect the properties of the final fiber, in terms of functional groups and composition.

1.2. Wood as raw material

Within natural and biodegradable sources, there are diverse feedstocks that can be used as cellulose sources such as sisal, linen, sugarcane bagasse, pineapple, straw, cotton, among others (Morán et al. 2008; Cherian et al. 2010; Abraham et al. 2011; Mandal and Chakrabarty 2011; Morais et al. 2013; Visanko et al. 2017). Centuries ago, in the pulp and paper industry, linen and cotton rags were used as the basic fiber sources. With the necessity to increase the production and to improve specific properties of paper, wood became the principal source of cellulose (Sjöström 1993; Sixta 2006).

Wood is an anisotropic and hygroscopic material, which chemical composition can vary with species, environment, age, geographic location, soil conditions, and weather (Pettersen and Rowell 1984).

Wood species can be divided in two groups commonly known as softwood (SW) and hardwood (HW). The former include pine and spruce, while examples of the later are birch and aspen. Based on the general amount of carbohydrates, lignin, and extractives of each class, it can be seen that have different chemical compositions (Table 1.1). In addition, as one of the main differences between them is the fiber length, in which softwood has longer fibers (~2-6 mm) while hardwoods have short fibers (~0.8-1.6 mm) (Solala 2011)

Table 1.1. Wood chemistry composition in percentage of dry wood weight (Sjöström 1993).

Wood	Cellulose	Hemicelluloses			Lignin	Extractives
		Galactoglucomannans	Xylan	Glucomannan		
SW*	37-43%	15-20%	5-10%	-	25-33%	2-5%
HW**	39-45%	-	15-30%	2-5%	20-25%	2-4%

*SW: Softwood, **HW: Hardwood

1.3. Constituents of wood

As mentioned previously, the main components fiber of wood are carbohydrates and lignin unevenly distributed along the cell wall layers (Figure 1). In wood structure, 65-70 % of the total dry weight is made up of cellulose and hemicelluloses, also known as holocellulose (Rowell et al. 2012). Understanding their structure and interactions within the fibers is crucial to understand how the pulping process will affect their final properties for further applications.

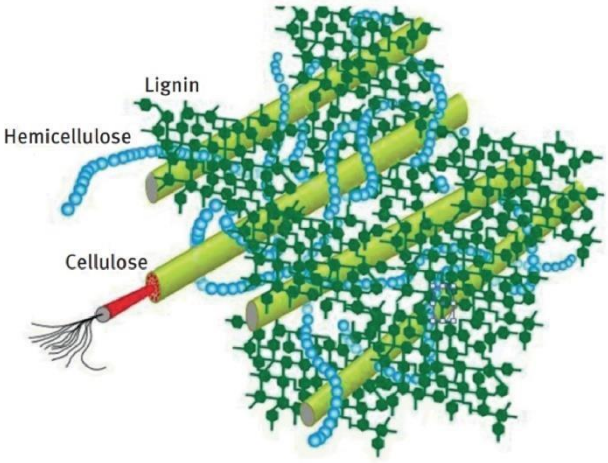

Figure 1.1. Wood components arrangement on the cell wall layers. Reprinted from Wang and Luo (2017) with permission from De Gruyter.

1.3.1. Cellulose

Cellulose is a linear homopolymer made up of β-D-glucopyranose units which are linked together by (1-4) glycosidic bonds (Sjöström 1993; O'Sullivan 1997). The repeating β-D-glucopyranose units, together with the OH groups of the carbon atoms in position 4 and 1 (C4 and C1), are covalently linked through acetal functions, making an extensive and linear polymer (Klemm et al. 2005). The repeating unit of cellulose is called cellobiose in which two sugar units are held together by a β-(1-4) glycosidic bonds (Figure 1.2).

Regarding the ends of the cellulose chain, C1 is the reducing end-group, the presence of a hemiacetal. On the other hand, C4 behaves as an aliphatic hydroxyl with a non-reducing end (Sixta 2006; Dufresne 2017). The OH groups present of the cellulose fibers structure give to this polymer certain polarity.

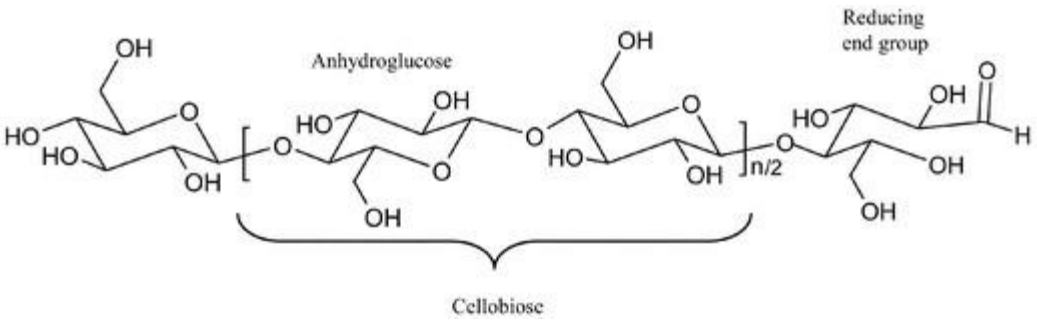

Figure 1.2. Cellulose chain structure. Reprinted from Kontturi et al. (2006) with permission from Royal Society of Chemistry.

Within the molecular structure of cellulose, each anhydroglucose unit has three OH groups linked to the carbons 2, 3, and 6, respectively (C2, C3, and C6). The three OH groups are able to interact with hydroxyl groups from other anhydroglucose units forming inter and intramolecular bonds within and between cellulose chains (Roman 2009) (Figure 1.3), conferring rigidity, stability, and water insolubility to the cellulose (Moon et al. 2011). Within these interactions, two are defined as intra-molecular H-bonds occurring from O(3)-H to O(5) and O(2)-H to O(6), and one inter-molecular H-bond taking place from O(3)-H to O(6)-H (Kontturi et al. 2003).

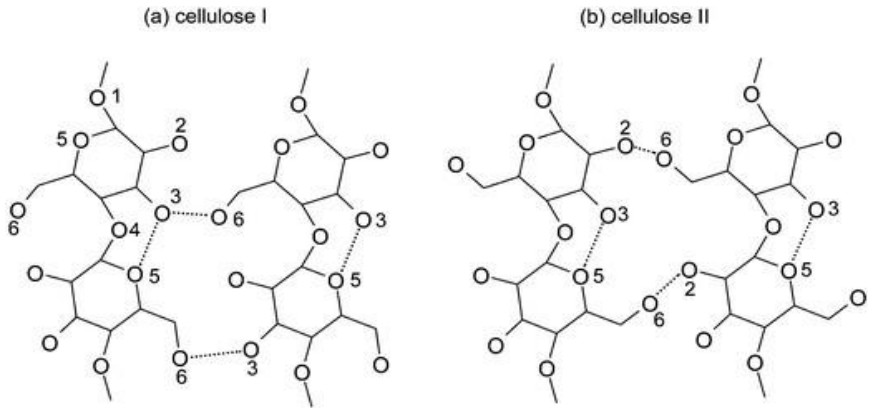

Figure 1.3. Intra and inter-molecular interactions within and between cellulose chains. Adapted from Kontturi et al. (2003) with permission from Royal Society of Chemistry.

Within the cell wall, cellulose can be found in two different forms known as crystalline and non-crystalline regions, also called amorphous or disordered; the former are typically non accessible to water, chemicals, or microorganisms while the latter are more easily accessible (Kondo et al. 2001; Rowell et al. 2012). Based on the arrangement and hydrogen bonds within and between the cellulose chains, different crystalline allomorphs cellulose I, II, III_I, III_{II}, IV_I, and IV_{II} exist that can be interconverted, by chemical or thermal treatments (Habibi et al. 2010).

Native cellulose is also known as cellulose I. Within its structure, the cellulose chains are organized in parallel, with two different crystalline forms, Iα and Iβ (Figure 1.4). The main difference between these is the hydrogen bonding patterns (Viëtor et al. 2000; Dufresne 2017). The importance of this packing resides in the fact that microfibrils formed by monoclinic cellulose will have different planes where hydroxyl groups will be highly concentrated with a specific hydrophobic plane (2 0 0) that can have an impact in the interactions of the fibrils with surrounding molecules (Koyama et al. 1997; Hult et al. 2003). The different pulping methods will have an

impact in this crystalline packing of the cellulose microfibrils. The chemicals utilized in the different treatments will interact with the fibrils for the removal of other cell wall components. The pulping chemicals will also penetrate the cellulose structure and rearrange it (Duchesne et al. 2001; Hult et al. 2001, 2003; Quiroz-Castañeda and Folch-Mallol 2013).

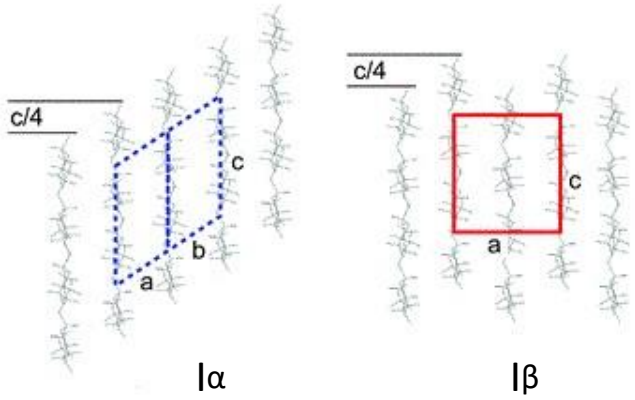

Figure 1.4. Hydrogen bonding patterns for Iα and Iβ. Adapted from Moon et al. (2011) with permission from Royal Society of Chemistry.

After cellulose is isolated from the cell wall, the interaction with specific chemicals will transform the native cellulose I crystals into different polymorphs. Cellulose II is the product of the re-crystallization of the chains after sodium hydroxide mercerization. During this process, intermediate conversion stages are reached, and different Na-cellulose compounds are formed. Finally, the mercerized cellulose is organized in an antiparallel mode (Revol and Goring 1981; Okano and Sarko 1984, 1985) which is the most stable allomorph (Kolpak et al. 1978; Kroon-Batenburg and Kroon 1997) (Figure 1.5). This process does not dissolve the cellulose chains but only leads to the swelling of the fibers (Dufresne 2017). Cellulose II can also be obtained by regeneration where hydrogen bonds need to be broken to solubilize the cellulose. For this purpose,

ionic liquids have been discovered to be effective alternatives (Swatloski et al. 2002; Turner et al. 2004; Brandt et al. 2013). Cellulose can then be precipitated in solvents such as water, acetone or ethanol (Zhu et al. 2006). Conversion reactions from cellulose I to II are irreversible, suggesting a higher thermodynamic stability based on the structure of cellulose II (Dufresne 2017). Cellulose III_I and III_{II} emerge after treatment of cellulose I and cellulose II, respectively, with ammonia, while cellulose IV_I and IV_{II} are obtained by heating cellulose III_I and III_{II}, respectively (Nelson and O'Connor 1964; Paakkari et al. 1989; O'Sullivan 1997; Kontturi et al. 2006; Habibi et al. 2010; Ioelovich 2016).

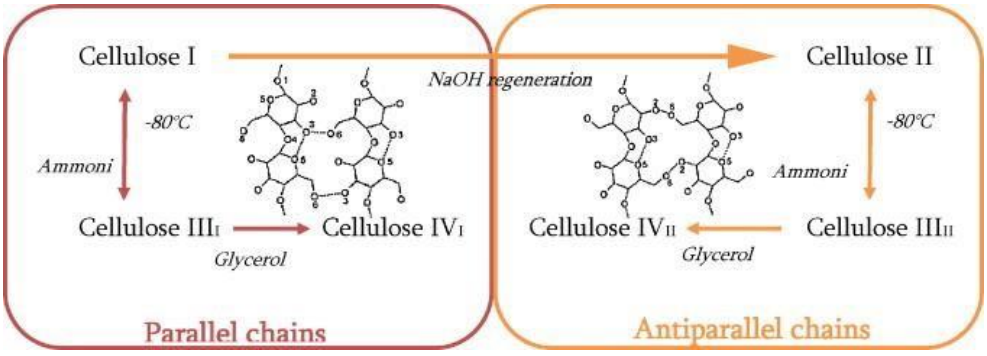

Figure 1.5. Polymorphs of cellulose and their obtaining sequence. Reprinted from Lavoine et al. (2012) with permission from Elsevier.

Cellulose is further organized forming elementary fibrils with diameters between 3-5 nm. Elementary fibrils are combined into larger structures called microfibrils with diameters between 10 to 20 nm, which are further arranged together in a fibril-matrix like structure mixed with hemicellulose and lignin that can be found on the cell wall layers (Postek et al. 2011). The fibril-matrix structures are treated by the previously mentioned pulping methods to obtain cellulose

fibers with diameters in the range of micrometers. Furthermore, through chemical, mechanical and/or enzymatic processing of the cellulose fibers, nanocelluloses can be obtained. Nanocelluloses are characterized by having at least one dimension within the nanoscale (Klemm et al. 2011). The higher surface area of the nanosized particles, provides unique surface properties. Additionally, the chemistry of the pulping method chosen will provide additional functional groups available for modifications, inducing changes in charge density, zeta potential and optical activity of such fibrils (Lagerwall et al. 2014; Salas et al. 2014). These unique varieties of properties, added to the inherent biocompatibility, biodegradability, sustainability, and renewability of lignocellulosic fibers, open a new set of opportunities to utilize these materials in novel fields as wide as environmental remediation, biomedical devices, electronics, construction, or energy storage.

1.3.2. Hemicellulose

Hemicelluloses are the second most important polysaccharide constituent in lignocellulosic materials, belonging to the heteropolysaccharides and are usually branched (Klemm et al. 2005; Tunc and Van Heiningen 2008). They can have different structures and properties depending on the species from which they were obtained. In addition, the hemicellulose content can vary between species, such as softwood and hardwood, as it was presented on Table 1.

Within hemicellulose, they can be divided in two large groups; pentoses which contain five carbons (e.g., xylose and arabinose) and hexoses formed by six carbons (e.g., glucose, galactose, mannose) (Rowell et al. 2012).

Hemicelluloses are branched and amorphous structures, usually constituted of different combinations of monomers, such as galactoglucomannans and glucuronoxylans. The less orderly arrangement of hemicelluloses compared with cellulose makes the former more accessible to

chemicals, water, or microorganisms (Li 2011). In addition, hemicelluloses have lower degrees of polymerization when compared with cellulose that makes them more soluble (Sjöström 1993).

By performing enzymatic hydrolysis, it has been demonstrated that hemicelluloses are mainly located between the cellulose microfibrils in the cell wall structure, while remaining hemicelluloses have been proposed to occur within the amorphous region of the cellulose microfibrils structure (Arola et al. 2013).

Although hemicelluloses and cellulose have an affinity (Eronen et al. 2011), the former can be also found covalently linked with lignin, leading to the occurrence of lignin-carbohydrates complexes (LCC) (Paszczyński et al. 1988). Thus, hemicelluloses have been proposed as the intermediate compound, which has affinity for both, lignin and cellulose.

A few studies have found that the presence of hemicelluloses play a significant role in the properties of cellulose fibers. First, they improve pulp fibrillation due to reduction of coalescence between the fibers (Duchesne et al. 2001; Hult et al. 2001; Iwamoto et al. 2008); and secondly, they tend to enhance the colloidal stability of a suspension due to the higher charge repulsion among the fibers (Hannuksela et al. 2003; Hubbe et al. 2008; Cheng et al. 2009; Tenhunen et al. 2014). As a result, the presence of hemicelluloses improves properties of the fibers such as thermal stability and strength (Iwamoto et al. 2008). Nevertheless, during the pulping process, a large amount of hemicellulose is degraded (Tunc and Van Heiningen 2008).

1.3.3. Lignin

Within the cell wall structure, lignin has been defined as the adhesive that holds together cellulose and hemicelluloses. Due to it hydrophobic character, it can be used to modify the hydrophilic ability of cellulose (Bian et al. 2018) Lignin can be described as an amorphous and branched polymer of phenylpropane units forming three-dimensional structures (Chakar and

Ragauskas 2004). These structures are made up by C-O-C and C-C linkages (Rowell et al. 2012) between the monolignols, *p*-coumaryl alcohol, coniferyl alcohol, and sinapyl alcohol (Sjöström 1993) (Figure 1.6).

As mentioned previously, lignin and polysaccharides can be linked together by covalent bonds, forming lignin-carbohydrates complexes (LCC) (Paszczyński et al. 1988), linked by ether, ester, or even glycosidic bonds (Paden et al. 1983; Sjöström 1993).

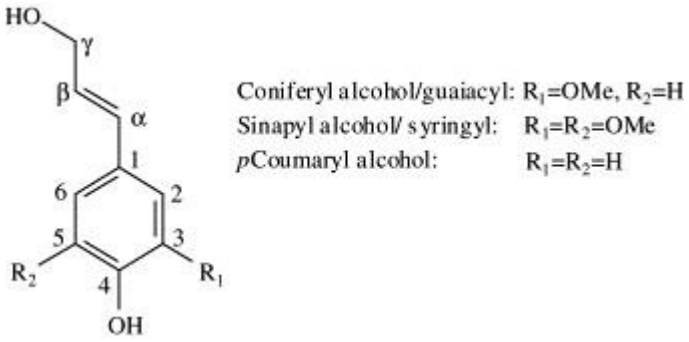

Figure 1.6. Three lignin precursors. Reprinted from Chakar and Ragauskas (2004) with permission from Elsevier.

Although lignin has been studied for decades, due to its complex structure and the changes this biomaterial undergoes after the pulping process, the exact original chemical structure of remains unknown.

1.4. Pulping methods

During wood pulping, the primary objective is to preserve the structure of wood fibers intact, while enhancing the removal of lignin as extensively as possible (Gratzl and Chen 1999;

Smook 2016b). Because of the different percentages of the wood components (Table 1), diverse methodologies have been developed for the removal of lignin and extractives, depending on their suitability to different species. Hemicelluloses are usually retained in different degrees according to the final end-use of the fibers and even thought the degree of polymerization is lower, hemicellulose contains a high amount of surface hydroxyl groups that can interact with the cellulose fibers or other materials (Suurnäkki et al. 1997; Hult et al. 2001; Toivonen et al. 2015).

Pulping methods can be classified in three principal categories: chemical, mechanical, and semi-chemical. The most commonly used chemical methods are kraft and acid sulfite. Even though the kraft and sulfite methods are the most used in the pulp and paper industries, organosolv extractions and enzymatic isolation are also important when non wood-based biomass are utilized as starting materials (Nascimento et al. 2014, 2016; Vallejos et al. 2016). Based on the method used to produce the cellulose fibers, they will be suitable for different applications as the fiber properties will be modified (Sixta et al. 2006).

During the chemical pulping process, lignin must be removed to allow the separation of cellulose fibers. When the removal of lignin reaches a certain value, the degradation of hemicelluloses and cellulose begin as undesired effects. Due to the undesired effects on the polysaccharides, chemical reactions have to be stopped to avoid the degradation of the carbohydrates (Sixta et al. 2006).

During the early 1970´s, a study compared the different pulping processes in terms of production in tons per year showing, at that time, the kraft process was responsible for about 78% over the total of pulp capacity (Kepple 1970). More recently, a study published by the Food and Agriculture Organization of the United States (FAO) estimated that in 2020, the kraft pulp production (bleached and unbleached) in the US will be 99.5% compared with a 0.5% for bleached sulfite pulping (Figure 1.7) (FAO 2016).

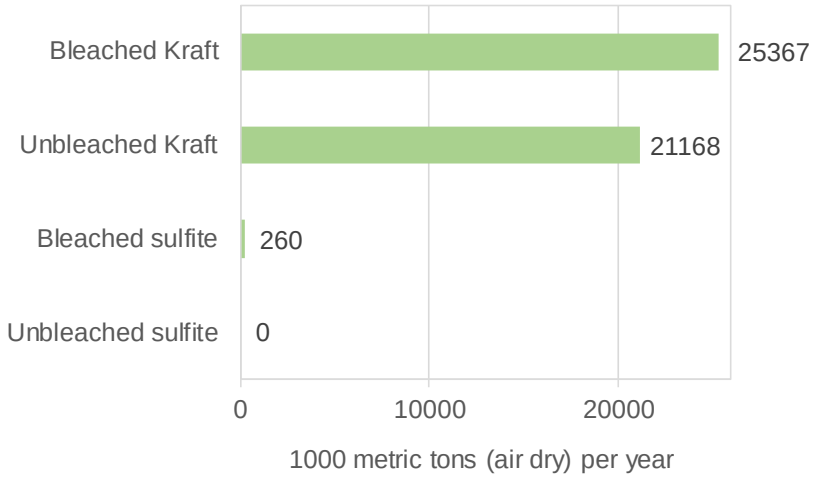

Figure 1.7. Estimated total capacity US pulp production (2020). Information adapted from FAO (2016).

1.4.1. Kraft pulping

In 1884, Carl Ferdinan Dahl patented the production of cellulose from wood, commonly known as kraft process. At that time, the cooking liquor contained sulfate of soda, soda carbonate, soda hydrate, and sodium sulfide (Dahl 1884). Over the years, this process has been modified and efficient alternatives have been developed. Currently, this alkaline method consists of a cooking liquor containing sodium hydroxide (NaOH) and sodium sulfide (Na_2S) with operational conditions ranging from 2 to 4 hours at temperatures between 170 – 180 ºC (Li 2011; Smook 2016c).

As an indicator of the prominence of the Kraft pulping, a more recent comparison between the amount of kraft and sulfite mills in North America in 2016 was made, showing that from a total of 100 mills, 95 used kraft process while only 5 used the sulfite process (Smook 2016a). The

increased tendency toward the utilization of kraft pulping over the other methods can be explained mainly by three factors; (1) efficient recovery of the chemicals, (2) good quality of the produced fibers, and finally, (3) the opportunity of using different types of woods (Kepple 1970).

During the kraft process, fibers are subjected to very alkaline conditions, high temperatures, and mechanical stress (Vänskä et al. 2016). The key reactions during this procedure involve the cleavage of lignin, where the rupture of the structure is mainly through the C-O-C linkages. Although, the active chemicals used are NaOH and Na_2S, the presence of hydrosulfide ions (HS^-), a product of the reaction between Na_2S with water, are mainly responsible for the lignin cleavage reactions (Smook 2016c). As a secondary effect during the kraft pulping, a higher aggregation of the fibers occurs during the initial step, increasing the diameter of the microfibrils (Hult et al. 2001, 2003) which has been proposed mainly be the result of the elimination of hemicelluloses and lignin, which allows greater contact between the fibers and thus, among the aforementioned OH groups.

1.4.2. Sulfite pulping

In 1866, Benjamin C. Tilghman patented his finding in pulping methodology establishing the bases for the production of delignified pulp from wood and fibrous materials (Phillips 1943). Currently, this process has been further studied and refined. The general concept is still based on the use of SO_2, obtained from $(HSO_3)^-$, for the modification of lignin, and the use of some cationic base (Ca^{+2}, Mg^{+2}, Na^+, NH_3^+) for the prevention of chromophores formation from the residual lignin on the fibers and its later hydrolysis. The difference in the cationic base allows the pulp to cook at a wider range of pH that can improve yield and properties of the fibers (Smook 2016a). Typical cooking is done at low pH (~1.5) which has the drawback that the integrity of the fibers

can be compromised due to hydrolysis reactions. The use of the alternative cationic bases helps to increase the pH up to 5. Standard operation temperatures range from 130 ºC to 140 °C for 6 to 8 hours and pressure of 100 psi (689.5 kPa) (Poletto et al. 2011; Smook 2016a).

Other modifications of the sulfite process have been developed ever since, mainly to increase the operational pH to reduce corrosion and improve the integrity of the fibers. Two processes are mostly used; neutral sulfite pulping and alkali sulfite which are mainly applied in semi-chemical processing were the sulfite process softens the fibers prior to the grinding of the pulps (Gümüşkaya and Usta 2006; Patt et al. 2006; Forouzanfar et al. 2016). The resulting semi-chemical pulps have a higher lignin content in order to improve yield rather than the complete isolation of the cellulose fibers.

At the present time, even when paper making is a large share of the final end product for sulfite pulps, the different surface properties of the fibers has marked a rapid increase of it use for dissolving pulps (Sixta 2000). Furthermore, there is an increase of its use for the utilization and consumption of wood derived materials (Quintana et al. 2015).

1.5. Effects of pulping on surface properties of cellulose fibers

1.5.1. Crystallinity

During the pulping processes, undesired reactions of the polysaccharides, such as peeling and hydrolysis are commonly occurring. These reactions are the result of interactions between OH^- ions, with (1) the reducing ends of the cellulose chains, and (2) at some random points on the cellulose chain (Strunk 2012).

In the case of cellulose, due to its high crystallinity and compact structure, there are fewer adverse effects, compared with hemicelluloses which due to their lower degree of polymerization

and branched structures are reduced approximately 40-50% during the early stages of the cooking process (Smook 2016b).

Analyzing the crystallinity in terms of the type of pulping process, it has been demonstrated that kraft pulps exhibit higher crystallinity than sulfite fibers as a result of the better fiber pack which can be correlated with their higher mechanical properties (Hult et al. 2001, 2003). Since sulfite pulping use strong acid conditions, the effects on the pulp super-molecular structure is mainly due to changes in the degree of polymerization and the polydispersity (PD) of the samples. This effect is a consequence of two aspects of the acidic pulping: i) the random hydrolysis, that is more common in sulfite process than in alkaline kraft process, and ii) the dissociation of the primary cell wall, which frees those smaller fibers from the bundles, while increasing the PD and inducing a lowering of the molecular weight in suspension (Sixta et al. 2006; Duan et al. 2015; Benítez and Walther 2017). During kraft pulping, a higher concentration of the $I\beta$ crystalline form is conserved, while during sulfite more $I\alpha$ are preserved, the latter of which have smaller length and diameter when compared with the cellulose from the kraft process, but being the aspect ratio of both in the same order of magnitude (Young 1994; Hult et al. 2002, 2003).

1.5.2. Surface functionalized groups

Another important effect that the pulping processes have over the fibrils is the functional groups that they will induce on the surface of the fibers. Such charged groups are related to many of the surface properties of the fibers and to their reactivity. Sulfite pulps have higher contents of carboxylic and carbonyl groups when compared to those of pretreated and non-pretreated kraft pulps (Young 1994; Sixta et al. 2006; Strunk 2012). Additionally, because of the use of sulfuric acid and its sulfite derivatives, sulphate groups occur on the fiber surface increasing their reactivity

and capability for further modification (Sjostrom and Enstrom 1966; Young 1994; Östenson et al. 2006).

During sulfite process, ether groups of lignin are cleaved by the acidic conditions of the medium and lignosulfonate compounds are formed due to the reaction of lignin with bisulfite ions ($HSO3^-$) (Smook 2016a). The presence of lignosulfonates promotes fiber swelling, making fibrillation and beating responses easier and faster since the fibrils have more repulsive interactions between them (Chakar and Ragauskas 2004). In papermaking, this surface functionality facilitates the interactions between different additives and the cellulose fibrils (Young 1994; Schwikal et al. 2011; Smook 2016b).

On the other hand, during kraft cooking process, hydroxide and hydrosulfide anions present in the white liquor are able to cleave lignin giving rise to the formation of free phenolic hydroxyl groups, which increase the hydrophilicity of lignin and consequently, its solubility (Chakar and Ragauskas 2004).

1.5.3. Chromophores groups

An additional and not necessarily desired consequence of the pulping methods during cooking is the formation of chromophoric groups responsible of the dark color of the fibers. During pulping process, oxidation reactions occurred converting the phenolic groups of lignin to quinone-like substances, which are the main responsibly of the absorption of light (Smook 2016d). Although chromophores groups occur in both types of pulps, while kraft is characterized by its dark color after pulping.

1.5.4. Lignin-carbohydrates complexes (LCC)

Other side reactions that occur during pulping are so-called condensation reactions, which are responsible for recombining and forming new C-C bonds, resulting in more insoluble compounds (Chakar and Ragauskas 2004). Additionally, while β-O-4 linkages of lignin are broken, new phenolic hydroxyl groups appear in the structure (Lawoko et al. 2005), resulting in fibers with a higher surface deposition of extractives and lignin, especially in the case of kraft pulps. Such effects can be explained by the higher alkaline conditions of the process and due to condensation reactions of the components (Shen and Parker 1999; Gustafsson et al. 2003).

Regarding the effects on the processes conditions, the higher the delignification, the lower the selectivity –in terms of cellulose yield- of the kraft process, and the higher the condensation reactions (Baptista et al. 2008). By lowering the concentration of hydroxide ions during kraft pulping, a higher carboxylate content can be reached, conferring higher tensile strength to the individual fibers (Dang et al. 2006).

1.5.5. General properties

Although kraft pulping had been widely adopted by the industry for its ease of chemical recovery, sulfite pulping allows a more efficient elimination of lignin, which impacts in the lignin solubility and consequently results in pulps that are easier to bleach (Hult et al. 2003; Smook 2016c, a).

The different types of hemicelluloses on wood are characterized for their impact in the fibers properties. Reports have shown that the kraft process retain a higher amount of xylose than sulfite pulping, but sulfite retains more mannose. When kraft pulp is pretreated, as is usually now for high-value pulps, such as dissolving pulp, then this relationship is inverted as the objective of the pretreatment is to eliminate the hemicellulose and improve the purity of the pulp (Sixta 2006;

Strunk 2012; Duan et al. 2015). Other important saccharide is glucose, which as the monomer of cellulose, was shown to be more conserved in sulfite pulping (in percentage ratios) (Hult et al. 2003; Strunk et al. 2012).

In both cases, the lignin content of sulfite pulp is always lower as the chemistry behind it improves the solubility and surface modification of the lignin polymer, which also generates different possibilities for the use of the residual stream (Page 1983; Fardim and Durán 2004; Rojo et al. 2015; Smook 2016a). On the other hand, brightness values are similar for the pretreated kraft and sulfite pulping methods (Sixta 2006; Strunk 2012).

Important findings regarding the coalescence of the fibers after the pulping processes have been reported. Alkaline sulfite pulps shown higher coalescence of fibers when compared to those neutral or acidic sulfite pulps, due to the effect of their surface functionalities (Hult et al. 2002, 2003; Pönni et al. 2012). As expected by the combination of chemical and mechanical processes, the neutral sulfite semi-chemical fibers (NSSC) show a higher content of lignin and hemicelluloses as the process is less focused on the pulp purity than in process yield, which has also been reported to be improved when compared with kraft pulps (Masura 1998; Shen and Parker 1999; Smook 2016a). Analyzing the surface energy, cellulose and lignin have surface energies of 56.6 mJ/m^2 and 48.2 mJ/m^2, respectively. Considering the surface energy of NSSC hardwood pulp and kraft hardwood pulp, it was found that they exhibit values close to those reported for cellulose (Shen and Parker 1999).

1.6. Bleaching process

Even when chemical pulping methods provide cellulose fibers with good mechanical properties, their lignin content is not low enough. Consequently, the implementation of bleaching

technology is needed in order to eliminate residual lignin without impacting the fibers mechanical properties (Sixta 2000; Smook 2016d).

The most commonly used oxidizing agents during the bleaching steps are chlorine dioxide (ClO_2), oxygen (O_2), ozone (O_3), and hydrogen peroxide (H_2O_2). The interaction of the fibers with oxidizing agents and alkaline washing cycles generate changes to the surface as these processes aim to modify the existing lignin while increasing its solubility.

Although bleaching processes are often used for pulp and paper production, among the main concerns are the environmental issues involving this practice. To address this, there has been a reduction in the use of chlorine and derivatives, in favor of the oxygen based methods (Serkov and Radishevskii 2009; Khakimova and Sinyaev 2014). Resultant pulps from this bleaching sequence are commonly known as Total Chlorine Free (TCF) pulps.

1.7. Surface properties after bleaching

Bleaching is normally done as a series of four to six steps usually based on an oxidative step followed by an alkali wash for the maximization of lignin solubility and removal. Depending on the choice of chemical used in each step, these sequences will then to produce fibers with different lignin contents. As an example, in a study published by Khakimova and Sinyaev (2014) six bleaching steps were performed on bisulfite pulp using the sequence: peroxide with sodium molybdate (acid medium) (Pa), alkali extraction (E), sodium chlorite (C_t), alkali extraction enriched with peroxide (E_P), and a final stage of sodium chlorite (C_t). This data showed 36.9 % delignification and a decrease of 1.8 μm in the mean width with also some loss in mechanical properties, which can be linked to the decrease in crystallinity (Khakimova and Sinyaev 2014). Similar processing but with chloride dioxide instead of C_t, showed a higher purity in sulfite derived

pulps than from those coming from pre-treated kraft, but more extractives remained in the surface of the sulfite pulp than in the kraft. This can be explained by the difference in surface reactivity, larger pores, and consequent water retention values (Duan et al. 2015).

Regarding the TCF method, this oxidative sequence is made up of oxygen delignification (O), an oxygen, peroxide enriched alkali extraction (EOP), followed by ozonation (Z), and a final enriched alkali extraction (EOP). In some cases the extraction stage can be enhanced with enzymes to eliminate hemicelluloses and amorphous cellulose as well as the residual lignin and lignin derived chromophores (Serkov and Radishevskii 2009; Quintana et al. 2015).

For the more traditional pulp and paper industry, the main finding was an impact to the fibers as a reduction in brightness and whiteness of the pulp obtained by TCF, even at the same levels of lignin content as in chlorine treated pulps. This reduction is proposed to be a consequence of the decrease in the molecular weight of the pulp during the ozone step. Smaller fiber size causes a decrease in the scattering coefficient, affecting the interaction of fibers with light and the brightness/whiteness and a subsequent increase of transparency of the fiber suspension. Even though this is an effect of ozonation, the base utilized in the previous alkali extraction stage has a strong influence in this outcome.

Bleaching processes have a direct impact on crystallinity of the cellulose fibers, with kraft fibers showing higher crystallinity, which is expected due to the removal of amorphous lignin and hemicelluloses (Popescu et al. 2008).

1.8. Nanocellulose

Based on renewable, biodegradable and biocompatible sources, lignocellulosic materials with nano-scale dimensions are known as nanocellulose. The methods applied to obtain

nanocellulose usually involve chemical-, mechanical-, and enzymatic treatments, or a combination thereof, giving rise to different types of nanocellulose types. Most commonly, the term nanocellulose refers to cellulose nanocrystals (CNC) and cellulose nanofibrils (CNF), the latter being the object of the present study. The main process to obtain CNC is based on acid hydrolysis of the cellulose fibers, where the less ordered regions of the fibrils are degraded (Habibi et al. 2010; Lu and Hsieh 2010; Postek et al. 2011). Carrying out this process, only the crystalline region of the fibers remain, forming rod-like structure, 10-2 nm in width and a several hundred nm in length (Xu et al. 2013). On the other hand, by performing a mechanical treatment, with or without enzymatic or chemical pre-treatment, both regions of the elementary fibrils remain in the structure, leading to the production of CNF. CNF particles are long flexible structures when compared with CNC, with similar or larger diameters (Xu et al. 2013).

Nanocellulose can be utilized in novel applications such as packaging, functional nanocomposites, emulsion stabilizers, as well as in the pharmaceutical and medical fields, due to their unique properties such as high aspect ratio, high strength, low density, and high capacity for chemical–modification (Spence et al. 2010; Klemm et al. 2011; Moon et al. 2011).

Particularly for the production of CNF, the chemical composition and properties of the starting lignocellulosic material will play an important role in the behavior of the resulting materials after fibrillation, as the individual components interact at a very fundamental level.

1.8.1. Cellulose nanofibrils (CNF)

During the early 1980s', Turbak et al. (1983) and Herrick et al. (1983) were the first to develop cellulose microfibrils (MFC) by homogenizing cellulose pulp suspensions under pressure. At that time, they found that beating and refining the cellulose pulp using only mechanical treatment was inefficient because large amounts of energy were needed to produce these small

particles, resulting in high production costs (Ankerfors 2012). However, during the last few decades, efforts have been focused on the development of different types of treatments along with the emergence of new technologies that have made it possible to obtain cellulose nanofibrils (CNF) in techno-economically feasible ways. Presently, the two most commonly used mechanical equipment to produce CNF are; (1) the microfluidizer, where the cellulose suspension is forced to pass through a small chamber allowing the fracture of the fiber into smaller portions (Lavoine et al. 2012), and (2) the supermasscolloider, where the suspensions are ground when passing between one stationary and one rotating stone which allows breaking and delamination of the fibers (Solala et al. 2012).

Today, nearly all CNF grades are produced from fully bleached chemical pulps that contain only trace amounts of residual lignin (<1%), which are called bleached cellulose nanofibrils (BCNF). Thus, the different processes to isolate lignin from the cellulose pulp, closely related with the further bleaching step, have been developed in order to eliminate the lignin content of the cellulose fibers as an initial step to obtain CNF, conferring to the cellulose nanofibrils different surface properties. Nevertheless, by changing the harshness of the pulping process, and restricting the use of bleaching steps, not all the lignin and hemicellulose present in the cellulose fibers need to be removed, providing new surface properties. Consequently, the nanocellulose made thereof, commonly known as lignin-containing cellulose nanofibrils (LCNF) will have improved properties such as lower water absorption and lower oxygen permeability (Ferrer et al. 2012; Rojo et al. 2015). Moreover, the use of LCNF, which contain not only lignin but also hemicelluloses, open new opportunities for its incorporation in diverse composite materials (Sun et al. 2014; Delgado-Aguilar et al. 2016; Ferrer et al. 2016; Wang et al. 2016). Furthermore, from an environmental point of view, the production of LCNF could be beneficial since the processes of lignin removal

as well as the following bleaching steps are no longer necessary (Rojo et al. 2015) contributing to a practice more friendly to the environment (Spence et al. 2010).

1.9. Conclusions

Herein it was shown how the two most important pulping methods have direct impact on the properties of the fibers, not only in mechanical, and structural, but in surface properties as well. Different impacts of the pulping processes have been pointed out as the main characteristics that affects the cellulose fibers, such as crystallinity, deposition of groups on the surface, and chromophores groups.

Kraft pulping is a very complex process in which variables such as time, chemical concentration, pH, and temperature, can be modified resulting in cellulose fibers with different properties. In addition, a wide variety of raw materials can be used, increasing the variability of the final properties of the material. Sulfite pulps have great surface availability, reactivity and better swelling properties than kraft pulps, making them ideal for dissolving pulps and for papermaking.

It is worth mentioning that both kraft and sulfite pulping are integrated procedures where not only chemical treatments are performed, but also several mechanical steps are used to improve the even distribution of chemicals and to get better dispersion of the fibers. While mechanical treatment is able to isolate the individual fiber components in different ways, chemical treatments modify the chemistry of its surface.

By adequately combining mechanical and chemical treatments during the production of cellulose fibers, desired properties can be imparted to the fibers. By knowing how the specific components of each raw material are modified after the pulping and bleaching process, a better

understanding of the subsequent cellulose nanofibers properties can be reached. Thus, this review provides a good overview of the work that has been performed in the area and to which properties attention should be drawn in order to better select them and improve the wide capability of the pulping of wood-based fibers.

References

Abraham E, Deepa B, Pothan LA, et al (2011) Extraction of nanocellulose fibrils from lignocellulosic fibres: A novel approach. Carbohydr Polym 86:1468–1475. doi: 10.1016/j.carbpol.2011.06.034

Ankerfors M (2012) Microfibrillated cellulose: Energy-efficient preparation techniques and key properties. Dissertation, KTH Royal Institute of Technology

Arola S, Malho J, Laaksonen P, et al (2013) The role of hemicellulose in nanofibrillated cellulose networks. Soft Matter 9:1319–1326. doi: 10.1039/C2SM26932E

Baptista C, Robert D, Duarte AP (2008) Relationship between lignin structure and delignification degree in Pinus pinaster kraft pulps. Bioresour Technol 99:2349–2356. doi: 10.1016/j.biortech.2007.05.012

Benítez AJ, Walther A (2017) Cellulose nanofibril nanopapers and bioinspired nanocomposites: a review to understand the mechanical property space. J Mater Chem A 16003–16024. doi: 10.1039/C7TA02006F

Bian H, Gao Y, Wang R, et al (2018) Contribution of lignin to the surface structure and physical performance of cellulose nanofibrils film. Cellulose 25:1309–1318. doi: 10.1007/s10570-018-1658-x

Brandt A, Gräsvik J, Hallett JP, et al (2013) Deconstruction of lignocellulosic biomass with ionic liquids. Green Chem 15:550–583. doi: 10.1039/c2gc36364j

Chakar FS, Ragauskas AJ (2004) Review of current and future softwood kraft lignin process chemistry. Ind Crops Prod 20:131–141. doi: 10.1016/j.indcrop.2004.04.016

Cheng Q, Wang S, Rials TG (2009) Poly(vinyl alcohol) nanocomposites reinforced with cellulose fibrils isolated by high intensity ultrasonication. Compos Part A Appl Sci Manuf 40:218–224.

doi: 10.1016/j.compositesa.2008.11.009

Cherian BM, Leão AL, de Souza SF, et al (2010) Isolation of nanocellulose from pineapple leaf fibres by steam explosion. Carbohydr Polym 81:720–725. doi: 10.1016/j.carbpol.2010.03.046

Dahl GF (1884) Process of manufacturing cellulose from wood. US Pat. 0,002,969 35 2

Dang Z, Elder T, Ragauskas AJ (2006) Influence of kraft pulping on carboxylate content of softwood kraft pulps. Ind Eng Chem Res 45:4509–4516. doi: 10.1021/ie060203h

Delgado-Aguilar M, González I, Tarrés Q, et al (2016) The key role of lignin in the production of low-cost lignocellulosic nanofibres for papermaking applications. Ind Crops Prod 86:295–300. doi: 10.1016/j.indcrop.2016.04.010

Duan C, Li J, Ma X, et al (2015) Comparison of acid sulfite (AS)- and prehydrolysis kraft (PHK)-based dissolving pulps. Cellulose 22:4017–4026. doi: 10.1007/s10570-015-0781-1

Duchesne I, Hult E, Molin U, et al (2001) The influence of hemicellulose on fibril aggregation of kraft pulp fibres as revealed by FE-SEM and CP/MAS13C-NMR. Cellulose 8:103–111. doi: 10.1023/A:1016645809958

Dufresne A (2017) Nanocellulose: From nature to high performance tailored materials, 2nd edn. De Gruyter, Germany

Eronen P, Österberg M, Heikkinen S, et al (2011) Interactions of structurally different hemicelluloses with nanofibrillar cellulose. Carbohydr Polym 86:1281–1290. doi: 10.1016/j.carbpol.2011.06.031

FAO (2016) Pulp and paper capacities. Rome

Fardim P, Durán N (2004) Retention of cellulose, xylan and lignin in kraft pulping of eucalyptus studied by multivariate data analysis: Influences on physicochemical and mechanical properties of pulp. J Braz Chem Soc 15:514–522. doi: 10.1590/S0103-50532004000400012

Ferrer A, Hoeger IC, Lu X, et al (2016) Reinforcement of polypropylene with lignocellulose nanofibrils and compatibilization with biobased polymers. J Appl Polym Sci 133:43584. doi: 10.1002/APP.43854

Ferrer A, Quintana E, Filpponen I, et al (2012) Effect of residual lignin and heteropolysaccharides in nanofibrillar cellulose and nanopaper from wood fibers. Cellulose 19:2179–2193. doi: 10.1007/s10570-012-9788-z

Forouzanfar R, Vaysi R, Rezaei VT, et al (2016) Study on production of fluting paper from poplar pulp mixed with hardwood NSSC pulp. J Indian Acad Wood Sci 13:55–63. doi: 10.1007/s13196-016-0166-6

Gratzl JS, Chen C-L (1999) Chemistry of Pulping: Lignin Reactions. Lignin Hist Biol Mater Perspect 742:392–421. doi: 10.1021/bk-2000-0742

Gümüşkaya E, Usta M (2006) Dependence of chemical and crystalline structure of alkali sulfite pulp on cooking temperature and time. Carbohydr Polym 65:461–468. doi: 10.1016/j.carbpol.2006.02.004

Gustafsson J, Ciovica L, Peltonen J (2003) The ultrastructure of spruce kraft pulps studied by atomic force microscopy (AFM) and X-ray photoelectron spectroscopy (XPS). Polymer (Guildf) 44:661–670. doi: 10.1016/S0032-3861(02)00807-8

Habibi Y, Lucia LA, Rojas OJ (2010) Cellulose nanocrystals: Chemistry, self-assembly, and applications. Chem Rev 110:3479–3500. doi: 10.1021/cr900339w

Hannuksela T, Fardim P, Holmbom B (2003) Sorption of spruce O-acetylated galactoglucomannans onto different pulp fibres. Cellulose 10:317–324. doi: 10.1023/A:1027399920427

Herrick FW, Casebier RL, Hamilton KJ, et al (1983) Microfibrillated Cellulose: Morphology and

Accessibility. J Appl Polym Sci Appl Polym Symp 37:797–813

Hubbe M, Rojas OJ, Lucia L, et al (2008) Cellulosic Nanocomposites: a Review. BioResources 3:929–980. doi: 10.15376/biores.3.3.929-980

Hult EL, Iversen T, Sugiyama J (2003) Characterization of the supermolecular structure of cellulose in wood pulp fibres. Cellulose 10:103–110. doi: 10.1023/A:1024080700873

Hult EL, Larsson PT, Iversen T (2001) Cellulose fibril aggregation - An inherent property of kraft pulps. Polymer (Guildf) 42:3309–3314. doi: 10.1016/S0032-3861(00)00774-6

Hult EL, Larsson PT, Iversen T (2002) A comparative CP/MAS13C-NMR study of the supermolecular structure of polysaccharides in sulphite and kraft pulps. Holzforschung 56:179–184. doi: 10.1515/HF.2002.030

Ioelovich MY (2016) Models of supramolecular structure and properties of cellulose. Polym Sci Ser A 58:925–943. doi: 10.1134/S0965545X16060109

Iwamoto S, Abe K, Yano H (2008) The effect of hemicelluloses on wood pulp nanofibrillation and nanofiber network characteristics. Biomacromolecules 9:1022–1026. doi: 10.1021/bm701157n

Kamel S (2007) Nanotechnology and its applications in lignocellulosic composites, a mini review. Express Polym Lett 1:546–575. doi: 10.3144/expresspolymlett.2007.78

Kepple PJ (1970) Kraft Pulping. TAPPI 53

Khakimova FK, Sinyaev KA (2014) Environmentally safe bleaching of bisulfite pulp. Russ J Appl Chem 87:1319–1325. doi: 10.1134/S1070427214090213

Klemm D, Heublein B, Fink HP, et al (2005) Cellulose: Fascinating biopolymer and sustainable raw material. Angew. Chemie - Int. Ed. 44:3358–3393

Klemm D, Kramer F, Moritz S, et al (2011) Nanocelluloses: A new family of nature-based

materials. Angew Chemie - Int Ed 50:5438–5466. doi: 10.1002/anie.201001273

Kolpak FJ, Weih M, Blackwell J (1978) Mercerization of cellulose: 1. Determination of the structure of Mercerized cotton. Polymer (Guildf) 19:123–131. doi: 10.1016/0032-3861(78)90027-7

Kondo T, Togawa E, Brown RM (2001) "Nematic ordered cellulose": A concept of glucan chain association. Biomacromolecules 2:1324–1330. doi: 10.1021/bm0101318

Kontturi E, Tammelin T, Österberg M (2006) Cellulose—model films and the fundamental approach. Chem Soc Rev 35:1287–1304. doi: 10.1039/B601872F

Kontturi E, Thüne PC, Niemantsverdriet JW (2003) Novel method for preparing cellulose model surfaces by spin coating. Polymer (Guildf) 44:3621–3625. doi: 10.1016/S0032-3861(03)00283-0

Koyama M, Helbert W, Imai T, et al (1997) Parallel-up structure evidences the molecular directionality during biosynthesis of bacterial cellulose. Proc Natl Acad Sci U S A 94:9091–9095. doi: 10.1073/pnas.94.17.9091

Kroon-Batenburg LMJ, Kroon J (1997) The crystal and molecular structures of cellulose I and II. Glycoconj J 14:677–690. doi: 10.1023/A:1018509231331

Lagerwall JPF, Schütz C, Salajkova M, et al (2014) Cellulose nanocrystal-based materials: from liquid crystal self-assembly and glass formation to multifunctional thin films. NPG Asia Mater 6:e80. doi: 10.1038/am.2013.69

Lavoine N, Desloges I, Dufresne A, et al (2012) Microfibrillated cellulose - Its barrier properties and applications in cellulosic materials: A review. Carbohydr. Polym. 90:735–764

Lawoko M, Henriksson G, Gellerstedt G (2005) Structural differences between the lignin-carbohydrate complexes present in wood and in chemical pulps. Biomacromolecules 6:3467–

3473. doi: 10.1021/bm058014q

Li J (2011) Isolation of lignin from wood. Dissertation, Saimaa University of Applied Sciences

Li MC, Wu Q, Song K, et al (2015) Cellulose Nanoparticles: Structure-Morphology-Rheology Relationships. ACS Sustain Chem Eng 3:821–832. doi: 10.1021/acssuschemeng.5b00144

Lu P, Hsieh YL (2010) Preparation and properties of cellulose nanocrystals: rods, spheres, and network. Carbohydr Polym 82:329–336. doi: 10.1016/j.carbpol.2010.04.073

Mandal A, Chakrabarty D (2011) Isolation of nanocellulose from waste sugarcane bagasse (SCB) and its characterization. Carbohydr Polym 86:1291–1299. doi: 10.1016/j.carbpol.2011.06.030

Masura V (1998) A mathematical model for neutral sulfite pulping of various broadleaved wood species. Wood Sci Technol 32:1–13

Moon RJ, Frihart CR, Wegner T (2006) Nanotechnology applications in the forest products industry. For Prod J 56:4–10. doi: 10.1126/science.102.2651.392

Moon RJ, Martini A, Nairn J, et al (2011) Cellulose nanomaterials review: structure, properties and nanocomposites. Chem Soc Rev Chem Soc Rev 40:3941–3994. doi: 10.1039/c0cs00108b

Morais JPS, Rosa MDF, De Souza Filho MDSM, et al (2013) Extraction and characterization of nanocellulose structures from raw cotton linter. Carbohydr Polym 91:229–235. doi: 10.1016/j.carbpol.2012.08.010

Morán JJI, Alvarez VVA, Cyras VPV, et al (2008) Extraction of cellulose and preparation of nanocellulose from sisal fibers. Cellulose 15:149–159. doi: 10.1007/s10570-007-9145-9

Nascimento DM, Almeida JS, Dias AF, et al (2014) A novel green approach for the preparation of cellulose nanowhiskers from white coir. Carbohydr Polym 110:456–463. doi: 10.1016/j.carbpol.2014.04.053

Nascimento DM do, Dias AF, Araújo Junior CP de, et al (2016) A comprehensive approach for obtaining cellulose nanocrystal from coconut fiber. Part II: Environmental assessment of technological pathways. Ind Crops Prod 93:58–65. doi: 10.1016/j.indcrop.2016.02.063

Nelson ML, O'Connor RT (1964) Relation of Certain Infrared Bands to Cellulose Crystallinity and Crystal Lattice Type. Part I. Spectra of Lattice Types I, II, III and of Amorphous Cellulose. J Appl Polym Sci 8:1311–1324

O'Sullivan AC (1997) Cellulose: The structure slowly unravels. Cellulose. doi: 10.1023/A:1018431705579

Okano T, Sarko A (1985) Mercerization of cellulose. II. Alkali–cellulose intermediates and a possible mercerization mechanism. J Appl Polym Sci 30:325–332. doi: 10.1002/app.1985.070300128

Okano T, Sarko A (1984) Mercerization of cellulose. I. X-ray diffraction evidence for intermediate structures. J Appl Polym Sci 29:4175–4182. doi: 10.1002/app.1984.070291247

Östenson M, Järund H, Toriz G, et al (2006) Determination of surface functional groups in lignocellulosic materials by chemical derivatization ESCA analysis. Cellulose 13:157–170. doi: 10.1007/s10570-005-5855-z

Paakkari T, Serimaa R, Fink H -P (1989) Structure of amorphous cellulose. Acta Polym 40:731–734. doi: 10.1002/actp.1989.010401205

Paden CA, Frank AS, Wieber JM, et al (1983) Properties of Wood Lignin. Acs Symp Ser 214:241–250. doi: 10.1021/bk-1983-0214.ch017

Page DH (1983) The origin of the differences between sulfite and kraft pulps. PULP Pap 84:TR15--TR20

Paszczyński A, Crawford RL, Huynh VB (1988) Manganese peroxidase of Phanerochaete

chrysosporium: Purification. Methods Enzymol 161:264–270. doi: 10.1016/0076-6879(88)61028-7

Patt R, Kordsachia O, Fehr J (2006) European hardwoods versus Eucalyptus globulus as a raw material for pulping. Wood Sci Technol 40:39–48. doi: 10.1007/s00226-005-0042-9

Pettersen RC, Rowell RM (1984) The Chemical Compostition of Wood. In: Rowell R (ed) The chemistry of solid wood. American Chemical Society, Washington, pp 57–126

Phillips M (1943) Benjamin Chew Tilghman, and the Origin of the Sulfite Process for Delignification of Wood. J Chem Educ 20:444. doi: 10.1021/ed020p444

Poletto M, Pistor V, Zeni M, et al (2011) Crystalline properties and decomposition kinetics of cellulose fibers in wood pulp obtained by two pulping processes. Polym Degrad Stab 96:679–685. doi: 10.1016/j.polymdegradstab.2010.12.007

Pönni R, Vuorinen T, Kontturi E (2012) Proposed nano-scale coalescence of cellulose in chemical pulp fibers during technical treatments. BioResources 7:6077–6108. doi: 10.15376/biores.7.4.6077-6108

Popescu CM, Tibirna CM, Raschip IE, et al (2008) Bulk and Surface Characterization of Unbleached and Bleached Softwood Kraft Pulp Fibres. Cellul Chem Technol 42:525–547

Postek MT, Vladár A, Dagata J, et al (2011) Development of the metrology and imaging of cellulose nanocrystals. Meas Sci Technol 22:024005. doi: 10.1088/0957-0233/22/2/024005

Quintana E, Valls C, Vidal T, et al (2015) Comparative evaluation of the action of two different endoglucanases. Part I: On a fully bleached, commercial acid sulfite dissolving pulp. Cellulose 22:2067–2079. doi: 10.1007/s10570-015-0623-1

Quiroz-Castañeda RE, Folch-Mallol JL (2013) Hydrolysis of Biomass Mediated by Cellulases for the Production of Sugars. In: Sustainable Degradation of Lignocellulosic Biomass. Intech, pp

119–155

Ratner BD, Hoffman AS, Schoen FJ, et al (2013) Biomaterials Science: An Introduction to Materials, Third Edit. Academic Press

Revol J -F, Goring DAI (1981) On the mechanism of the mercerization of cellulose in wood. J Appl Polym Sci 26:1275–1282. doi: 10.1002/app.1981.070260419

Rojo E, Peresin MS, Sampson WW, et al (2015) Comprehensive elucidation of the effect of residual lignin on the physical, barrier, mechanical and surface properties of nanocellulose films. Green Chem 17:1853–1866. doi: 10.1039/C4GC02398F

Roman M (2009) Model Cellulosic Surfaces: History and Recent Advances. Model Cellul Surfaces 1019:3–53. doi: doi:10.1021/bk-2009-1019.ch001

Rowell R, Pettersen R, Tshabalala M (2012) Cell Wall Chemistry. In: Handbook of Wood Chemistry and Wood Composites, Second Edition. pp 33–72

Salas C, Nypelö T, Rodriguez-Abreu C, et al (2014) Nanocellulose properties and applications in colloids and interfaces. Curr. Opin. Colloid Interface Sci. 19:383–396

Schwikal K, Heinze T, Saake B, et al (2011) Properties of spruce sulfite pulp and birch kraft pulp after sorption of cationic birch xylan. Cellulose 18:727–737. doi: 10.1007/s10570-011-9526-y

Serkov AA, Radishevskii MB (2009) Effect of bleaching without chlorine on the change in the optical properties of pulp in grinding. Fibre Chem 41:307–313. doi: 10.1007/s10692-010-9194-y

Shen W, Parker IH (1999) Surface composition and surface energetics of various eucalypt pulps. Cellulose 6:41–55. doi: 10.1023/A:1009268102404

Sixta H (2006) Raw material for pulp. In: Sixta H (ed) Handbook of Pulp. WILEY-VCH Verlag

GmbH &Co. KGaA, Weinheim, Lenzing Austria, pp 21–61

Sixta H (2000) Comparative evaluation of TCF bleached hardwood dissolving pulps. Lenzinger Berichte 79:119–128

Sixta H, Potthast A, Krotschek AW (2006) Chemical Pulping Processes. In: Handbook of Pulp. pp 109–229

Sjöström E (1993) Wood chemistry-fundamentals and applications, 2nd edn. Academic Press Inc., San Diego

Sjostrom E, Enstrom B (1966) A method for separate determination of sulpho and carboxyl groups in sulphite pulps. Sven Papperstidning-nordisk Cellul 69:55

Smook G (2016a) Sulfite pulping. In: Kocurek M (ed) Handbook for Pulp and Paper Technologists, 4th edn. TAPPI Press, Georgia, pp 68–74

Smook G (2016b) Handbook for Pulp and Paper Technologists, 4th edn. TAPPI Press, Georgia

Smook G (2016c) Kraft Pulping. In: Kocurek M (ed) Handbook for Pulp & Paper Technologist, 4th edn. TAPPI Press, Georgia, pp 76–85

Smook G (2016d) Bleaching. In: Kocurek M (ed) Handbook for Pulp & Paper Technologist, 4th edn. TAPPI Press, Georgia, pp 167–181

Solala I (2011) Mechanochemical reactions in lignocelluloseic materials. Dissertation, Aalto Universty

Solala I, Volperts A, Andersone A, et al (2012) Mechanoradical formation and its effects on birch kraft pulp during the preparation of nanofibrillated cellulose with Masuko refining. Holzforschung 66:477–483. doi: 10.1515/HF.2011.183

Spence KL, Venditti RA, Rojas OJ, et al (2010) The effect of chemical composition on microfibrillar cellulose films from wood pulps: Water interactions and physical properties for

packaging applications. Cellulose 17:835–848. doi: 10.1007/s10570-010-9424-8

Strunk P (2012) Characterization of cellulose pulps and the influence of their properties on the process and production of viscose and cellulose ethers. Dissertation, Umeå University

Strunk P, Lindgren Å, Agnemo R, et al (2012) Properties of cellulose pulps and their influence on the production of a cellulose ether. Nord Pulp Pap Res J 27:24–34. doi: 10.3183/NPPRJ-2012-27-01-p024-034

Sun H, Wang X, Zhang L (2014) Preparation and characterization of poly(lactic acid) nanocomposites reinforced with Lignin-containing cellulose nanofibrils. Polym 38:464–470. doi: 10.7317/pk.2014.38.4.464

Suurnäkki A, Tenkanen M, Buchert J, et al (1997) Hemicellulases in the bleaching of chemical pulps. Adv Biochem Eng Biotechnol 57:261–87. doi: 10.1007/BFb0102077

Swatloski RP, Spear SK, Holbrey JD, et al (2002) Dissolution of cellulose with ionic liquids. J Am Chem Soc 124:4974–4975. doi: ja025790m [pii]

Tenhunen TM, Peresin MS, Penttilä PA, et al (2014) Significance of xylan on the stability and water interactions of cellulosic nanofibrils. React Funct Polym 85:157–166. doi: 10.1016/j.reactfunctpolym.2014.08.011

Toivonen MS, Kurki-Suonio S, Schacher FH, et al (2015) Water-Resistant, Transparent Hybrid Nanopaper by Physical Cross-Linking with Chitosan. Biomacromolecules 16:1062–1071. doi: 10.1021/acs.biomac.5b00145

Tunc MS, Van Heiningen ARP (2008) Hemicellulose extraction of mixed southern hardwood with water at 150 ^{o}C: Effect of time. Ind Eng Chem Res 47:7031–7037. doi: 10.1021/ie8007105

Turbak A, Snyder F, Sandberg K (1983) Microfibrillated cellulose. US Pat 4,374,702 11:1–11. doi: 10.1145/634067.634234.

Turner MB, Spear SK, Holbrey JD, et al (2004) Production of bioactive cellulose films reconstituted from ionic liquids. Biomacromolecules 5:1379–1384. doi: 10.1021/bm049748q

Vallejos ME, Felissia FE, Area MC, et al (2016) Nanofibrillated cellulose (CNF) from eucalyptus sawdust as a dry strength agent of unrefined eucalyptus handsheets. Carbohydr Polym 139:99–105. doi: 10.1016/j.carbpol.2015.12.004

Vänskä E, Vihelä T, Peresin MS, et al (2016) Residual lignin inhibits thermal degradation of cellulosic fiber sheets. Cellulose 23:199–212. doi: 10.1007/s10570-015-0791-z

Viëtor RJ, Mazeau K, Lakin M, et al (2000) A priori crystal structure prediction of native celluloses. Biopolymers 54:342–354. doi: 10.1002/1097-0282(20001015)54:5<342::AID-BIP50>3.0.CO;2-O

Visanko M, Sirviö JA, Piltonen P, et al (2017) Mechanical fabrication of high-strength and redispersible wood nanofibers from unbleached groundwood pulp. Cellulose 24:4173–4187. doi: 10.1007/s10570-017-1406-7

Wang C, Kelley SS, Venditti RA (2016) Lignin-based thermoplastic materials. ChemSusChem 9:770–783. doi: 10.1002/cssc.201501531

Wang S, Luo Z (2017) Pyrolysis of Biomass. De Gruyter, Berlin

Xu X, Liu F, Jiang L, et al (2013) Cellulose nanocrystals vs. Cellulose nanofibrils: A comparative study on their microstructures and effects as polymer reinforcing agents. ACS Appl Mater Interfaces 5:2999–3009. doi: 10.1021/am302624t

Young RA (1994) Comparison of the properties of chemical cellulose pulps. Cellulose 1:107–130. doi: 10.1007/BF00819662

Zhu S, Wu Y, Chen Q, et al (2006) Dissolution of cellulose with ionic liquids and its application: a mini-review. Green Chem 8:325. doi: 10.1039/b601395c

Chapter 2

The effect of lignin and hemicellulose on the properties of cellulose nanofibrils suspensions

2.1. Introduction

Since the emergence of nanotechnology, the possibility of bringing cellulose to the nanoscale has been a research topic of increased interest for various proposed applications. In papermaking industry (Espinosa et al. 2016), these applications include its use in paper coating (Hult et al. 2010; Missoum et al. 2013) and as additive to increase paper strength (Taipale et al. 2010; Vallejos et al. 2016). Nanocellulose is also being used as rheological modifier (Dimic-Misic et al. 2013; Li et al. 2015a; Liu et al. 2017a), as reinforcement particle in composite materials (Lee et al. 2009, 2014; Kajanto and Kosonen 2012), as packaging materials with improved barrier properties (Spence et al. 2010; Belbekhouche et al. 2011; Rojo et al. 2015), as an emulsion stabilizer (Cunha et al. 2014), and as an additive for medical and pharmaceutical products for control drug release and diagnostics (Tong et al. 2018).

The two most important types of nanocellulose for which production processes and yields have been highly optimized over the years are referred to as cellulose nanocrystals (CNC) and cellulose nanofibrils (CNF). By utilizing biomass as the raw material, CNC and CNF can be obtained by different approaches. The method frequently used to produce CNC, also known as cellulose whiskers, involves a strong acid hydrolysis in which the less ordered regions of the

elementary fibrils of cellulose are degraded, resulting in a highly crystalline nanomaterial (Postek et al. 2011; Xu et al. 2013; Chen et al. 2016; Bian et al. 2017b).

Alternatively, CNF is mainly produced by mechanical treatment of the raw material resulting in the disintegration of both crystalline and amorphous regions into nanoscale particles. It was during the early 1980'when the production of microfibrilar cellulose (MCF) was developed, using a high pressure homogenizer to fractionate the cellulose fibers to smaller sizes (Herrick et al. 1983; Turbak et al. 1983). During this process, the suspension was forced to pass several times through the equipment, resulting in energy consumptions over 25000 KWh per ton (Klemm et al. 2011). This bottleneck resulted in the development of pre-treatments, such as carboxymethylation (Wågberg et al. 1987), TEMPO-mediated oxidation (Saito et al. 2007; Isogai et al. 2011), and enzymatic pre-treatments (Henriksson et al. 2007; Pääkko et al. 2007) helping to easily delaminate the fiber, thereby consuming less energy (Siró and Plackett 2010). Although chemical and enzymatic pre-treatments have been developed to produce CNF, they are not strictly necessary (Zimmermann et al. 2010; Diop et al. 2017; Horseman et al. 2017), and the elimination of the strong chemical treatments needed to obtain CNC, is what turns the production of CNF into a more interesting alternative from an environmental and economic point of view (Abbati de Assis et al. 2017).

Currently, nearly all CNF grades are produced from fully bleached chemical pulps that contain only trace amounts of residual lignin (<1 %) and hemicelluloses, which are called bleached cellulose nanofibrils (BCNF). Different processes such as kraft and sulfite (Wang et al. 2016) in addition to pulp bleaching have been developed to eliminate the lignin content from the cellulose fibers as an initial step of CNF production. The required energy consumption during the mechanical treatment together with the lower yields of the process result in high CNF processing

costs as well as environmental impact. Consequently, CNF competitivity with other materials in the market at an industrial scale is compromised.

The use of unbleached cellulose pulps as starting material to produce lignin-containing cellulose nanofibrils (LCNF) which contain not only lignin but also hemicelluloses represents an interesting alternative for many applications due to the attractive properties conferred to the final materials (Rojo et al. 2015). From an economic and environmental point of view, the production of LCNF could be beneficial since the processes of lignin removal as well as the following bleaching steps are no longer necessary (Spence et al. 2010; Rojo et al. 2015). Moreover, with an emphasis on the mechanical treatment as the main method of LCNF production, it has been demonstrated that the presence of lignin improves the defibrillation process (Lahtinen et al. 2014). This improvement can be attributed to both the lignin and the hemicellulose content, which increase the surface charge of the material, resulting in repulsion between the fibrils thus allowing an easier separation from each other (Rojo et al. 2015).

During the last few years, more efforts have been directed to incorporate LCNF in different composite materials, employing a number of matrices such as polylactic acid (Sun et al. 2014; Wang et al. 2014), starch (Ago et al. 2016), polypropylene (Ferrer et al. 2016), polycaprolactone (Herzele et al. 2016), polystyrene (Ballner et al. 2016), and polyurethane (Visanko et al. 2017). Additionally, its utilization as adhesive replacement in wood composites (Diop et al. 2017), additive in papermaking (Delgado-Aguilar et al. 2016), and in composites films (Horseman et al. 2017) open new possibilities for this lignocellulosic nanoparticle.

Characterizing LCNF is essential for understanding not only the structure of the colloidal suspensions, but also the interactions between the different components of the structure, and how those materials interact when they are combined with others. Moreover, rheological properties are

of the highest importance since knowing the flow characteristics of the material may help during handling and processing (Agoda-Tandjawa et al. 2010; Nazari et al. 2016; Hubbe et al. 2017).

In the last few decades, the increasing interest on the rheological properties of CNF suspensions has been accompanied by the growth on the literature regarding this topic. Researchers have been studying the rheology of micro- and nano-scale cellulose fibrils (MFC and CNF, respectively) produced in different ways; e.g. by enzymatic treatments (Pääkko et al. 2007), from different raw materials (Rezayati Charani et al. 2013; Benhamou et al. 2014) or by applying different treatments to the fibers (Naderi et al. 2014). It is worth mentioning, that rheological characteristics of nanocellulose are mainly related to their intrinsic properties, such as the dimension and shape of the elements (rod-like structures for CNC and fibrillar structures for CNF), how branched or crystalline the structures are, and the surface charges of the nanoparticles (Guan Gong 2014).

As a general rheological behavior, it has been reported that CNF aqueous suspensions follow a shear thinning behavior (Herrick et al. 1983; Pääkko et al. 2007; Agoda-Tandjawa et al. 2010; Iotti et al. 2011; Karppinen et al. 2011; Tanaka et al. 2015). Shear thinning is a non-linear phenomenon in which the viscosity of the material decreases with increasing shear rate ($\dot{\gamma}$) due to the molecular motion of a polymer chain, surrounded by other molecular chains. Thus, when a deformation is applied, the whole polymer chains can only move in one direction, along their axis (Macosko 1994). Orientation of the particles during flow of the suspension is an important effect since they can agglomerate, align or even form networks that will have a direct impact on their viscosity (Hubbe et al. 2008).

The most common physical aspects affecting the rheological properties of CNF are solid content, temperature, pH, morphology, and surface charge (Pääkko et al. 2007; Agoda-Tandjawa et al. 2010; Iotti et al. 2011). The effect of the solid content on the viscosity can be explained by

analyzing the entanglements of the fibers (Iotti et al. 2011; Li et al. 2015b; Liu et al. 2017b). Higher concentrations of the suspensions bring on more entangled structures which increases the contact point between fibers and fibrils; the more chemical bonds among the fibrils, the higher the viscosity (Iotti et al. 2011). An additional change in the viscosity can be achieved by modifying the temperature of the system. This additional energy introduced on the structure is able to break down some bonds between the fibers resulting in decreased viscosity of the suspensions (Iotti et al. 2011). Regarding the pH of the slurries, it has been proved that pH significantly affects the rheological properties of CNF suspensions (Pääkko et al. 2007). The effect of charge density over bleached cellulose nanofibrils regarding their rheological behavior has also been studied, showing an increase of the viscosity as the charge density increases (Liu et al. 2017b).

In this work, we analyzed the rheological behavior of lignin-containing cellulose nanofibrils (LCNF) through steady state and oscillation modes. Divergence between samples was initially found as a result of different chemical compositions based on the amount of lignin and hemicelluloses present in the fibrils. To decrease the variability between samples, all LCNF consistencies and pH were adjusted to 1.5 wt. % and ~7.5, respectively. The influence of the charge of fibers on their rheological behavior was studied by analyzing the zeta-potential and their charge density. Microscopy analyses were carried out to achieve a better understanding of the effect of the morphology of the fibrils on their rheological behavior.

2.2. Optimization CNF production with Masuko Supermasscolloider

The production of CNF by mechanical treatment using a Masuko Supermasscolloider (MKZA10-15J - Masuko Sangyo Co., Fiber, Japan) (Figure 2.1) was optimized.

Prior to the production of cellulose nanofibrils, cellulose pulps need to be properly washed following a combination of steps to enhance its cleaning and subsequent optimal defibrillation. This process can be divided in two principal steps as described below.

Figure 2.1. Masuko Supermasscolloider (MKZA10-15J) acquired by Dr. Maria Soledad Peresin.

STEP 1: To eliminate all possible metallic particles present on the cellulose pulp a pre-washing using hydrochloric acid (HCl) is performed. Fibers are submerged in a solution 0.01 M for 30 min at pH = 2. Then, the cellulose pulps are washed using deionized water (DI) until pH = 5 to avoid the degradation of the fibers (Ferrer et al. 2012).

STEP 2: A washing step using sodium bicarbonate ($NaHCO_3$) is performed in order to convert the fibers to their sodium form. This washing step will favor the delamination between the fibrils and consequently will improve the defibrillation process and the quality of the product. Cellulose fibers were submerged in a $NaHCO_3$ solution 0.001 M. Sodium hydroxide (NaOH) (10 w/w %) was used to reach a pH = 9 in which the fibers were washed for 30 min. Further washing of the

cellulose pulp in DI water needs to be done to eliminate the excess reagent until the conductivity of the filtrate reaches 2 µS/cm (Ferrer et al. 2012).

Regarding the operation of the equipment, alumina or silica stones with different mesh size can be used to improve the fibrillation process. Additionally, depending on each sample, the gap between the stones can be selected, a parameter which is essential to obtain a good CNF quality.

2.3. Materials and methods

2.3.1. Raw material

For the purpose of this work, four different never-dried cellulose pulps were used. *Eucalyptus globulus* chips were supplied by La Montañanesa pulp mill (Torraspapel - Lecta Group, Spain), and the pulping process of the raw material was carried out by the National Institute of Agricultural and Food Research and Technology (INIA, Spain). The raw material was air dried and storage in polyethylene bags at 25 ºC until use. Kraft cooking was performed in a 26 L batch reactor furnished with a system for recirculation and heating of the cooking liquor. The cooking temperature was controlled by a computer running specially developed software. Cooking conditions were: 2 Kg of dry chips, 5 L/Kg liquor to wood ratio, 16 % active alkali (AA), 20 % sulfidity, 165 ºC cooking temperature, and 65 minutes to maximum temperature. Time at maximum temperature was varied to obtain an H-factor of 150 for pulp 4 and 460 for the rest of the pulps. The H-factor was calculated according to the following equation:

$$H = \int_0^t e^{\left(43.2 - \frac{16115}{T}\right)} dt \qquad (1)$$

in which T is the temperature (K) and t the time (hours).

After the cooking process was completed, the chips were discharged into the blowing tank, washed, disintegrated, and screened to remove uncooked material.

After cooking until H factor equal to 460, one third of the material was separated and named as pulp 3. The remaining material was subjected to oxygen delignification in a 20 L rotary reactor with a jacket-type electrical heater controlled by a computer to set and maintain the treatment temperature. Conditions of oxygen delignification were 110 ºC, 60 minutes, 0.6 MPa of oxygen pressure, 4 % NaOH o.d.p. (over dry pulp), 0.7 % MgSO4 o.d.p., and 8 % consistency.

After oxygen delignification, a half of the material was separated and named as pulp 2. The remaining pulp, named pulp 1, was bleached with hydrogen peroxide in the same reactor described above for oxygen delignification. Operational conditions were: 5 % H_2O_2 o.d.p., 2 % NaOH o.d.p., 1 % DTPA o.d.p., 0.2 % $MgSO_4 \cdot 7H_2O$ o.d.p., 8 % consistency, 90 ºC temperature, and the treatment duration was 120 minutes. Cooking conditions for each sample are summarized in Table 2.1. Cellulose pulps were then characterized as is explained in the following section.

Table 2.1. Cooking conditions of the cellulose pulps used to produce LCNF.

Sample	**Pulp 1**	**Pulp 2**	**Pulp 3**	**Pulp 4**
Dry chips (Kg)	2	2	2	2
Liquor/wood (L/Kg)	5	5	5	5
AA (%)	16	16	16	16
Sulfidity (%)	20	20	20	20
Cooking temperature (ºC)	165	165	165	165
Time until max. temperature (min)	65	65	65	65
H factor	460	460	460	150
Oxygen delignification	Yes	Yes	No	No
Bleaching	Yes	No	No	No

2.3.2. Characterization of the raw material for LCNF production

Chemical composition of the original wood chips and cellulose pulps made thereof was determined by standard analytical methods (National Renewable Energy Laboratory NREL/TP510-42618) and they are summarized in Table 2.2. After removing ethanol extractives, the sugar composition was determined by high performance liquid chromatography (HPLC) in an Agilent Technologies 1260 HPLC fitted with a refractive index detector (Agilent, Waldbronn, Germany) using an Agilent Hi-PlexPb column operated at 70 ºC with Milli-Q water as a mobile phase pumped at a rate of 0.6 mL/min. The solid residue remaining after acid hydrolysis is referred to as acid insoluble lignin (Klason lignin). Acid soluble lignin was quantified using UV-spectrophotometry at 205 nm.

2.3.3. LCNF Production

Cellulose nanofibrils were produced at the VTT Technical Research Center of Finland Ltd. (Espoo, Finland). Never-dried cellulose pulps were first diluted to approximately 1.8 wt. % following by a mechanical dispersion to avoid the formation of agglomerates. Afterwards, cellulose nanofibrils suspensions were obtained by using a combination of different mechanical processes. First, cellulose pulp in water was ground using a Supermasscolloider friction grinder MKZA10-15J (Masuko Sangyo Co., Fiber) by passing the suspension two times between one stationary and one rotating stone, allowing the break down and delamination of the fibers. Then, the suspensions already grounded in the Masuko were forced to pass five times through a small chamber of a Microfluidizer M7115-30 (Microfluidics Corporation), allowing the fracture of the fibers into smaller portions. Finally, gel-like nanocellulose suspensions were obtained from all the samples.

2.3.4. Self-standing LCNF films

Self-standing LCNF films were made by solvent casting method (Figure 2.3). LCNF suspensions prepared at 0.1 wt. % were sonicated for 10 min using a sonicator tip with 20 KW and 25 % of amplitude with a cold bath to avoid heating of the samples. Then, suspensions were placed inside polystyrene plastic Petri dishes and dried until films detached themselves from the surface. Films were then chemically and thermally characterized using attenuated total reflectance Fourier-transform infrared spectroscopy (FT-IR) and thermogravimetric analysis (TGA), respectively, as described below.

2.3.5. Characterization of LCNF suspensions

2.3.5.1. Zeta-potential

The colloidal stability of the suspensions was assessed by performing zeta potential measurements. For this purpose, pH and zeta-potential of the samples were measured using a SympHony Benchtop Multi Parameter Meter B30PCI (VWR®).

2.3.5.2. Average molar mass measurement

Average molar mass was measured by high-performance size exclusion chromatography (SEC). For these measurements, the solid samples were dissolved in DMAc/8 % LiCl according to the solvent exchange method described by Berthold et al. (2001). The samples were filtered through 0.45 µm syringe filter before the measurement. SEC analyses were performed using 2 x PL gel MiniMixed A columns with a pre-column in DMAc/LiCl eluent (0.36 ml/min) at T = 80 °C. The eluates were detected using Waters 2414 Refractive index detector. The molar mass distributions (MMD) were calculated against 8 x pullulan (6,100 - 708,000 g/mol) standards, using Waters Empower 3 software.

2.3.5.3. Thermogravimetric Analysis (TGA)

Thermogravimetric analysis was carried out to determine the thermal decomposition of the samples containing different amounts of lignin. Analyses were performed on a Perkin Elmer Pyrin 1 TGA. Samples were pre-heated at 30 ºC for 1 min followed by a heating rate of 10 ºC/min from 30 ºC up to 800 ºC in a nitrogen atmosphere (20 ml/min). Ceramic crucibles were used for all the measurements and the size of samples was approximately 5 mg for all the LCNF. Finally, all measurements were run in duplicate.

2.3.5.4. Fourier-transform infrared spectroscopy with attenuated total reflectance accessory (ATR-FTIR)

To determine chemical and structural composition of the samples, ATR-FTIR analyses were performed using a ThemoFisher Scientific – Nicolet 6700 FT-IR equipped with diamond ATR accessory. Before the measurements, a background spectrum was recorded for each different sample. Afterwards, all spectra were collected from 400 to 4000 cm^{-1} with a 2 cm^{-1} wavenumber resolution after 64 continuous scans. Data was processed using a OMNIC Software.

2.3.5.5. X-ray powder diffraction (XRD)

XRD analyzes were performed using a 1-Dimension Bruker AXS D8 Discover equipped with a LYNXE detector and Cu Kα irradiation. Measurements were performed at a scan speed of 0.1 second/step, from 5 to 90 degrees, and at continuous scan. Data was acquired using the EVA Software. The crystalline index (CI) was calculated using Segal's method (Segal et al. 1959) defined as:

$$CI = \frac{I_{200} - I_{Am}}{I_{200}} \times 100\% \quad (2)$$

where I_{200} is the maximum intensity of the 200 lattice diffraction peak, and I_{Am} is the intensity scattered by the amorphous fraction of the sample. Samples used were self-assembly films as described above.

2.3.5.6. Microscopy

The morphology of the samples was studied using optical microscopy, field emission scanning electron microscopy (FE-SEM), and atomic force microscopy (AFM).

For the optical microscopy, fibrillated samples were dyed using 0.5 % Congo red solution in a 1:1 ratio, followed by mixing of the solution to improve the coloration of the fibers. Then, the dyed suspension was mixed with water on the microscope slide (ratio 1:2). Measurements were performed using an Olympus BX-50 microscope equipped with a SensiCam 12BIT COLLED IMAGING.

For SEM imaging, LCNF suspensions were prepared at 0.1 wt. % and sonicated for 10 min using a sonicator tip with 20 KW and 25 % of amplitude to promote delamination and prevent their agglomeration. For this purpose, a cold bath was used to avoid heating of the samples. Afterwards, a droplet from each sample was placed onto a silica wafer air-dried for a few days. Before the measurement, surfaces were coated with a gold layer under an argon atmosphere using an EMS 550X Sputter Coating Device. SEM analyses were performed using a Carl Zeiss Supra 35VP SEM; images were taken with an accelerating voltage of 20 KeV at a working distance of ~ 7 mm.

For AFM imaging, LCNF suspensions were prepared at 0.01 wt. %, sonicated for 10 min using a sonicator tip with 20 KW and 25 % of amplitude with a cold bath. Suspensions were

deposited onto a silica surface by spin coating technique. Before the LCNF deposition, surfaces were cleaned using UV ozone for 30 min and submerged for 15 min into 0.1 wt. % polyethylenimine (PEI) which was used as anchoring solution. Images were obtained in tapping mode using a Bruker (formerly Digital Instruments, Veeco) AFM Dimension 3100 (California, US). Amplitude images were obtained at 2.35 Hz, and tip velocity of 23.4 µm/s using a Nano World (Innovative Technologies) FM 20 silicon SPM-sensor cantilever with resonance frequency of 75 kHz and force constant of 2.8 N/m. Images were processed with Gwyddion software 2.49 (SourceForge). Size of all images was 5 µmx5 µm.

The diameter of fibrils and fibers in each LCNF analyzed with AFM was determined by using the ImageJ software (Kimura et al. 1999). One hundred measurements were taken per AFM image, and the results of the measurements were then classified in nine different groups, according to the size range. For each size group, an average size value and its standard deviation was calculated (Figure 2.10).

2.3.5.7. Rheological behavior

Rheological measurements were carried out using a stress-controlled rheometer DHR-3 (TA Instruments) in a plate-plate geometry of 40 mm of diameter maintaining a constant temperature of 25 ºC.

Before measurements, LCNF suspensions were sonicated for 10 min using a sonicator tip with 20 KW and 25 % of amplitude using a cold bath to avoid heating of the samples. After sonication, all samples were thoroughly stirred using the spoon-end of a spatula (spoon-end: 32 x 14 mm, spatula-end: 51 x 7.9 mm) prior to loading. In all experiments, approximately 5 ml of sample were loaded using the spatula on the Peltier plate (Figure 2.2.a). The upper plate was lowered to 1050 µm gap. For optimal accuracy, trimming was done at this gap instead of the final

gap of 1000 µm. Sample in excess was trimmed followed by cleaning the surroundings using a Kim-wipe. At the final gap, silicon oil was delicately applied using a disposable pipette around the parallel plate to seal the system and prevent water evaporation (Figure 2.2.b). A flow test and oscillatory test were carried out. Once the measurements were finished, the upper plate was raised and only the sample containing 10.2 % of lignin was observed to remain attached to it (Figure 2.2.c).

For the flow curves, a pre-shear of 100 s^{-1} was applied during 5 min, with measurement done in triplicate and the averaged.

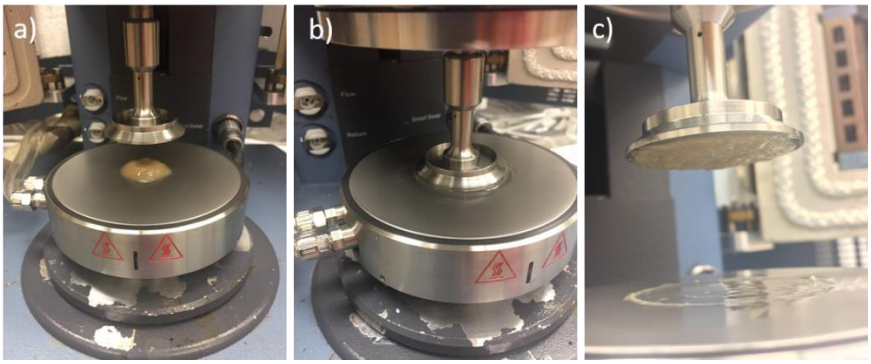

Figure 2.2. Rheological measurements of LCNF samples; a) load, b) oil barrier, and c) after measurement 10.2% LCNF remained attached to the upper plate.

2.3.5.8. Surface contact angle measurements (SCA)

Contact angle measurements were performed using the Ramé-Hart Standard Goniometer Model Nº 200-00-115 Serial Nº 502151 system (New Jersey, USA) equipped with an imaging system. Determination of the SCA was based on the analysis of the shape of the droplet and was performed with the software provided by the manufacturer (software version SCA 20.2.0).

For SCA analysis, LCNF suspensions were prepared at 0.01 wt. %, sonicated for 10 min using a sonicator tip with 20 KW and 25 % of amplitude with a cold bath. Suspensions were deposited onto a silica surface by spin coating technique. Before the LCNF deposition, surfaces were cleaned using UV ozone for 30 min and submerged for 15 min into 0.1 wt. % polyethylenimine (PEI) which was used as anchoring solution. Finally, the interaction between water and the different LCNF was measured by SCA.

2.4. Results and discussion

2.4.1. Wood characterization of the raw material for LCNF production

Chemical composition of both, wood chips and cellulose pulp made thereof, were analyzed in terms of the amounts of extractives, Klason lignin, soluble lignin, glucose, xylose, and arabinose content. Results are presented in Table 2.2.

Table 2.2. Wood chips and cellulose pulps quantification results expressed as percentage of analyzed sample

Sample	Extractives	Klason Lignin	Soluble Lignin	Total Lignin	Glucose	Xylose	Arabinose
Chips	2.0±0.1	22.0±0.9	4.6±0.1	26.6±1.0	47.8±0.3	15.7±0.3	0.8±0.0
Pulp 1	0.1±0.1	0.0±0.4	0.6±0.0	0.6±0.3	78.9±0.5	17.9±0.1	0.0±0.0
Pulp 2	0.1±0.0	0.9±0.6	0.8±0.0	1.7±0.6	77.9±0.1	18.5±0.1	0.0±0.0
Pulp 3	0.3±0.1	2.8±0.2	1.9±0.0	4.7±0.2	75.2±0.5	18.7±0.4	0.1±0.1
Pulp 4	0.7±0.1	6.8±0.2	3.3±0.0	10.2±0.2	77.9±0.0	20.8±0.0	0.3±0.0

Table 2.2 shows the variations in chemical compositions based on the changing of the H factor. As can be observed, lignin was reduced from 26.6 % in the original raw material to 0.6 % for the sample containing the less amount of lignin.

2.4.2. Self-standing films

The solvent casting method was successfully used as a technique to produce self-standing films. As can be observed in Figure 2.3, films containing the highest amount of lignin seem to have the smoothest surfaces. This can be attributed to; (1) the presence of lignin, which acts as a cementing material filling the void spaces between the fibrils, (2) the presence of hemicelluloses, specifically xylose, which as was presented on Table 2.2, remain on the fibers structure in important amounts and they can also fill the void spaces, and (3) the reduction of OH superficial groups on the cellulose fibers due to the higher lignin content. Nevertheless, this should be confirmed by using contact angle measurements and/or atomic force microscopy.

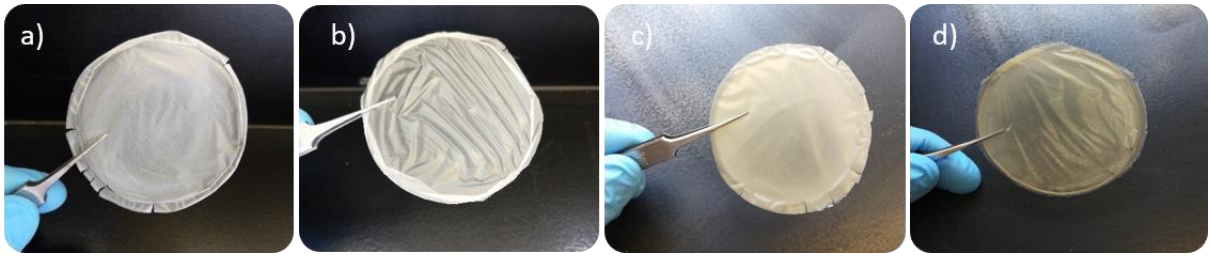

Figure 2.3. LCNF self-standing films made by solvent casting, a) 0.6, b) 1.7, c) 4.7, and d) 10.2 % of lignin.

2.4.3. Characterization of LCNF suspensions

2.4.3.1. Zeta-potential

Zeta-potential measurements give an indication of the stability of the colloidal suspensions. It is assumed that suspension with zeta-potentials higher than +30 mV or lower than -30 mV are stable (Herrera et al. 2018). Zeta potential for all the LCNF samples was measured at three different pH; 5, 7.6, and 9, and they are reported on Table 2.3.

Table 2.3. Characterization results of LCNF.

pH	5	7.6	9
Sample (lignin content)	**Zeta-potential (mV)**		
0.6 %	79.3	-71.3	-150.5
1.7 %	81.9	-72.4	-154.0
4.7 %	82.7	-71.1	-153.4
10.2 %	79.9	-72.3	-153.4

Analyzing the obtained results, although the samples had different amount of lignin and hemicelluloses on their composition, zeta-potential values do not change considerably between them at the same pH. At pH = 7.6 all had similar zeta-potential values of approximately -71 mV. Okita et al. (2010) measured the zeta-potential for different TEMPO-oxidized bleached CNF suspensions at pH = 8 reaching values of $\sim$ -75 mV for all the samples. As zeta-potential is directly related to the surface density of the dissociated carboxyl groups (Isogai et al. 2011) two assumptions can be made; (1) all the samples had the same density of carboxylic groups onto the fibrils surface and (2) lignin does not contribute to the zeta-potential measurements. A large

variation of the zeta-potential was observed as the pH of the samples changed. This suggest that pH has the highest impact on this property.

2.4.3.2. Molecular Weight Analysis

Molecular weight measurements were successfully assessed and the results can be observed in Table 2.4.

Table 2.4. Results from size exclusion chromatography for LCNF.

	Units	**Samples**			
Sample (lignin content)	%	0.6	1.7	4.7	10.2
Mn	kDa	65.4	71.9	60.1	89.6
Mw	kDa	349.6	499.8	599.4	624.4
PDI	-	5.3	6.9	9.9	6.9

Mn, number average molecular weight. Mw, average molar mass. PDI, polydispersity index.

Results in Table 2.4 show that Mw followed a trend regarding the amount of lignin; the higher the lignin content of the samples, the higher their molecular weight. These results could be attribute since the lower pulping treatment of the samples, they components are less degraded; thus, the degree of polymerization should be higher. Regarding the LCNF containing 4.7% of lignin, the Mn value is the lowest, showing a deviation from the previous mentioned trend. As mentioned above, samples are heterogeneous due to the presence of, not only cellulose, but also hemicellulose and lignin. Thus, the size of the particles has a higher variation, which can be confirmed by the PDI value of this sample. Regarding the standard, the utilization of pullulan for cellulose has been already investigated (Potthast et al. 2015). However, the presence of lignin in our samples could affect the obtained results. Besides, it has been reported on the literature the

utilization of tetrahydrofuran (THF) to dissolve lignin (Hage et al. 2009; Sevastyanova et al. 2014) while in our work DMAc/LiCl was used. Being aware of these assumptions is useful to understand why the differences between the measurements, the limitations of the technique based on the analyzed sample, which will be beneficial for further analysis.

2.4.3.3. Thermogravimetric Analysis (TGA)

Thermograms were collected for all the samples in duplicate. Although not reproducibility was obtained, results of only one measurement for each sample are shown in Figure 2.4. Data started to be stored at 30 ºC, however it is assumed that from 30 ºC to 120 ºC the weight loss corresponds to the elimination of moisture of the samples (Horseman et al. 2017).

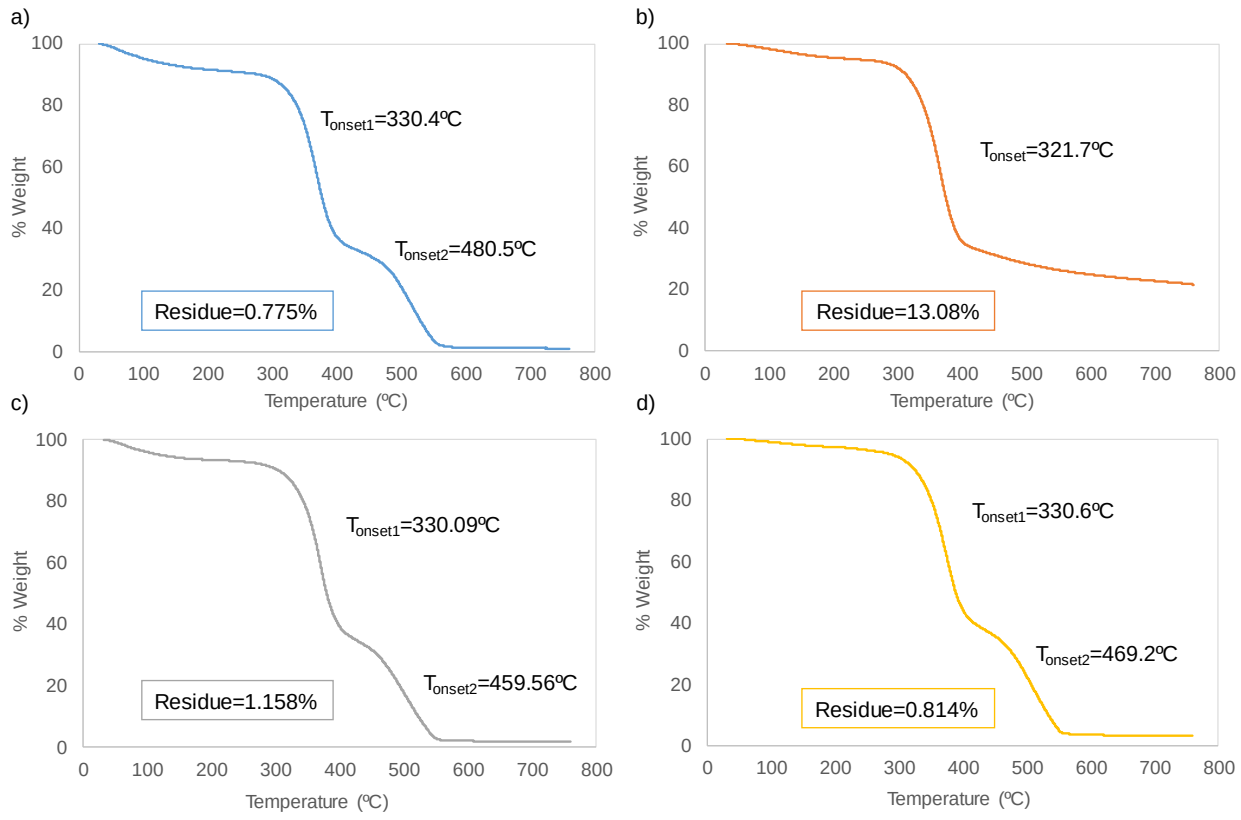

Figure 2.4. Thermal stability of LCNF samples containing; a) 0.6, b) 1.7, c) 4.7, and d) 10.2% lignin

Comparing the thermograph a) and b) from Figure 2.4 even when their chemical composition is very similar, it can be observed how their thermal decomposition is different.

The derivatives of the samples can be observed in Figure 2.5. Nevertheless, as in the case of Figure 2.4, results are not comparable since there lack of reproducibility.

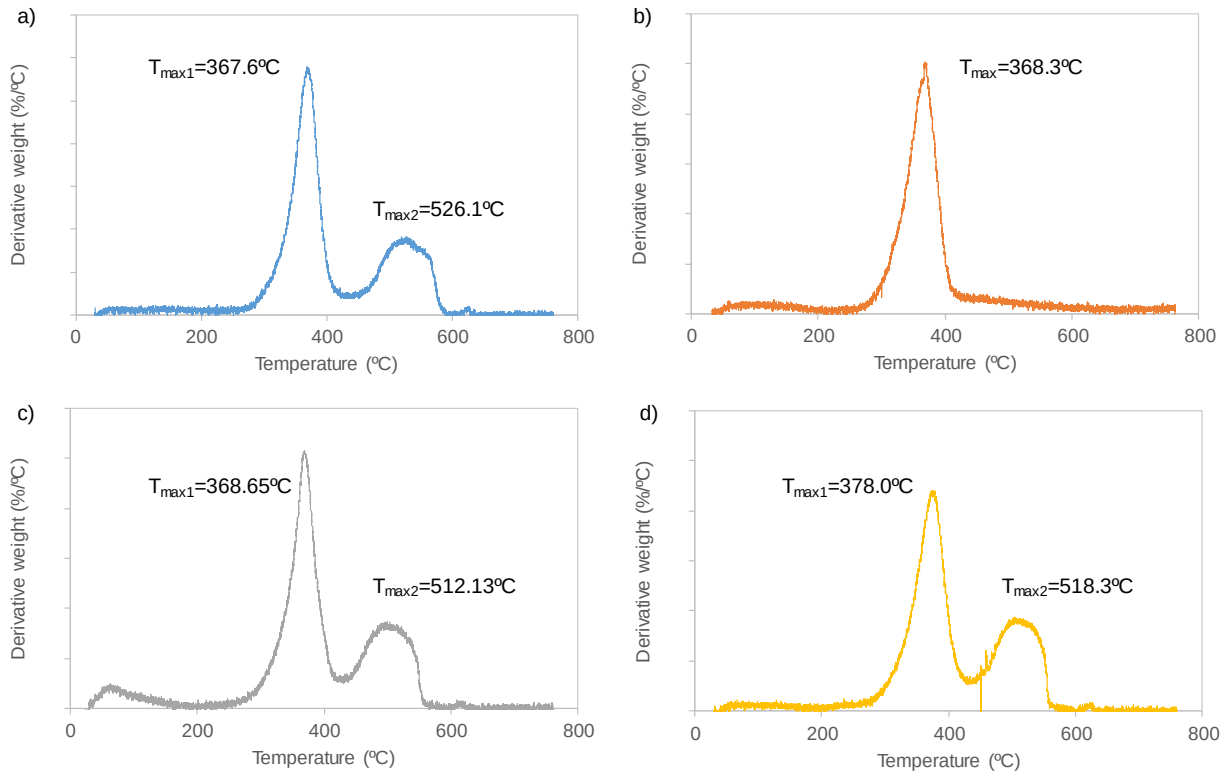

Figure 2.5. Derivative weight for LCNF containing; a) 0.6, b) 1.7, c) 4.7, and d) 10.2% lignin

It has been reported in the literature that lignin decomposes slower and in a broader range (between 160 to 900 ºC) than hemicelluloses and celluloses which have maximum peaks at 270 ºC and 360 ºC, respectively (Yang et al. 2007; Brebu and Vasile 2010). One of the reasons why lignin degradation occurs in a broader range of temperature is due to the different compounds this

polymer forms under pyrolysis conditions. At temperatures between 350-450 ºC, phenols groups on lignin structure are pyrolyzed and converted to pyrocatechols (Murwanashyaka et al. 2001). Additionally, at temperatures between 500-600 ºC, secondary reactions occur due to the decomposition of lignin intermediates (Brebu and Vasile 2010). Nevertheless, these results are not comparable since there lack of reproducibility. Samples were dried in different ways to obtain as much uniformity as possible. However, results were not in agreement between each other. Such inconsistency in reproducibility of the results is speculated to be caused by degradation of the samples over time.

Thermogravimetric measurements were performed using N_2 atmosphere. Thus, we should be able to observed a higher residue when the measurements ended, since there is not combustion of the sample. In a recent publication, similar results showing little amount of residue by using N_2 were presented (Diop et al. 2017). We suggest an entrance of air in the equipment while the measurement were running which could be the responsible for the combustion of the sample. Nevertheless, measurements will be repeat using other equipment to further investigate the behavior of the samples.

The two most important parameters that should be analyzed after the thermogravimetric analyses are the T_{max}, which is the maximum temperature value of the derivative curve (dm/dT), and the T_{onset}, that is defined as the temperature at which the loss mass becomes more apparent (Nair et al. 2017) and they are informed on Figure 2.4 and Figure 2.5, respectively.

2.4.3.4. Fourier-transform infrared spectroscopy with attenuated total reflectance accessory (ATR-FTIR)

Figure 2.6 shows the FT-IR spectra for the LCNF samples. All the spectra are very similar since no chemical treatment was performed on the cellulose nanofibrils. The absorption peak

corresponding to the aromatic and aliphatic O-H stretching vibrations (around 3327 cm^{-1}) seems to be slightly smaller for the sample containing the highest amount of lignin. This difference could be attributed to the reduction of the free –OH groups on the cellulose fibers surface as the lignin content increases (Diop et al. 2017). Besides, during kraft pulping the number of phenolic groups increase on the fibers as result of the elimination of lignin, which is in agreement with the peak at 3327 cm^{-1}. The peak located between 2800 and 2900 cm^{-1} correspond to C-H stretching due to aliphatic and aromatic structures (Yang et al. 2007). Analyzing the fingerprint region, at 1600 cm^{-1} there is an absorbance peak corresponding to the aromatic skeletal vibrations together with C=O stretching, corresponding to the presence of lignin (Huang et al. 2016). This can be corroborated on Figure 2.5 whereas the lignin content on the samples increase, the peak becomes sharper. The absorption peaks at 1436, 1378, and 1322 cm^{-1} are the result of CH_2, C-H, and O-H deformations respectively (Larkin 2011). At lower wavenumbers, absorbance peaks appearing at 1165 cm^{-1} are the result of C-O-C stretching due to the presence of the pyranose ring on the cellulose fiber structure; peaks at 1105 and 1034 cm^{-1} correspond to C-OH stretching (Yang et al. 2007) and C-O stretching vibration of lignin and polysaccharides (Huang et al. 2016). Finally, the absorbance peak at 895 cm^{-1} is associated with the C-C stretching (Yang et al. 2007).

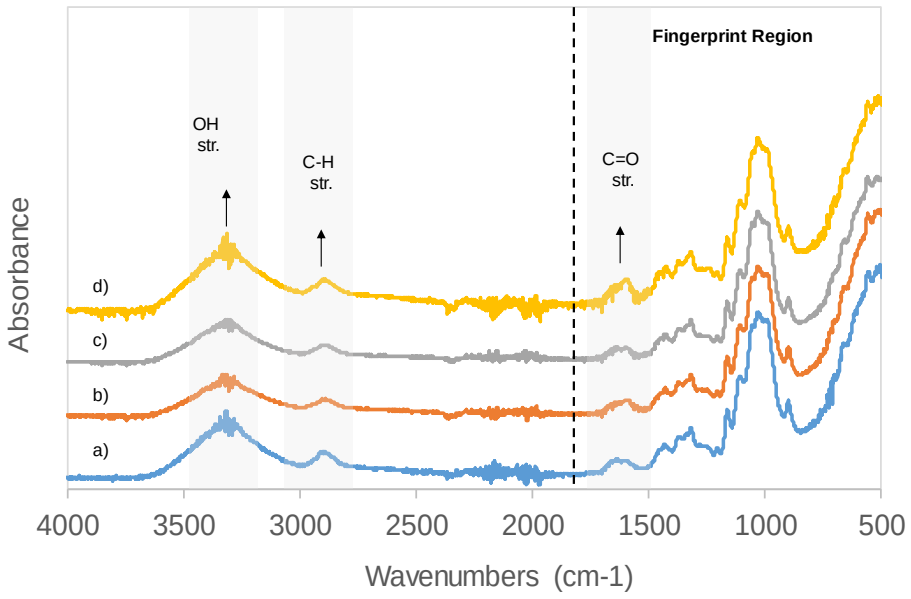

Figure 2.6. FT-IR spectra of the LCNF containing a) 0.6, b) 1.7, c) 4.7, and d) 10.2 % of lignin.

The spectra were normalized by taking as reference the more pronounced peak at 1034 cm^{-1} which, as mentioned above, correspond to the C-O stretching vibration of lignin and polysaccharides. However, in order to gain better definition of the spectra an increase the number of scans per spectra will be needed.

2.4.3.5. X-ray powder diffraction (XRD)

X-ray powder diffraction is a useful technique to calculate the crystallinity of the samples. XRD spectra are presented on Figure 2.7 and the crystallinity index was calculated based on the spectra using Segal's model (Eq. 2). All the samples have a major peak at a 2Θ value between 22.5º and 21.5º, and a smaller peak around 15.5º.

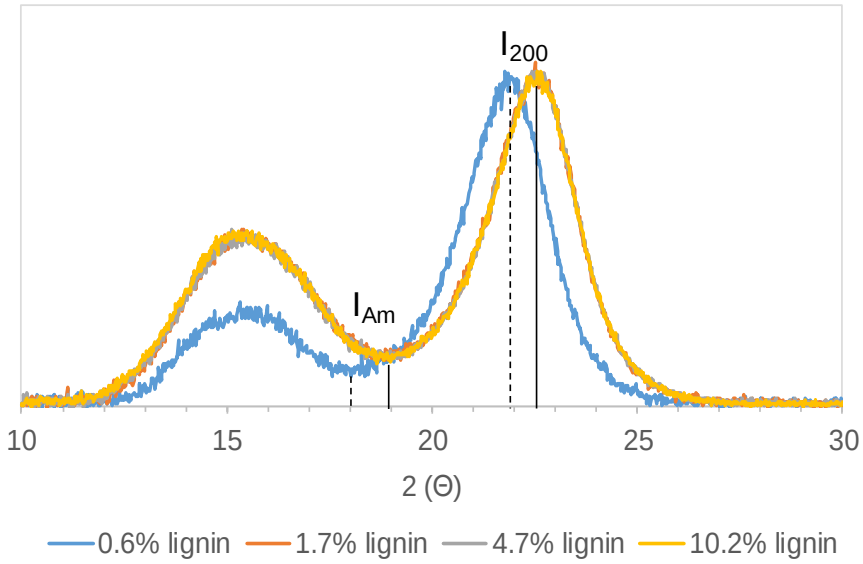

Figure 2.7. XRD spectra of LCNF samples.

The crystallinity index for the samples containing 0.6, 1.7, 4.7, and 10.2 % of lignin was found to be 91 %, 86.5 %, 86.3 %, and 87.1 %, respectively. As can be observed the samples seem to follow a pattern in which as the lignin content decreases, the crystallinity index increases, although the sample containing 10.2 % of lignin does not follow this behavior. By considering such differences negligible, this pattern could be explained due to the presence of lignin and hemicellulose which are characterized for having disordered and amorphous structures when compared with the well organized and compact cellulose crystals (Jonoobi et al. 2015).

2.4.3.6. Microscopy

Morphology of the samples was studied by using different techniques. Optical microscopy was used as the initial step (Figure 2.8). Although this method does not allow for the analysis of the material in the nano-scale, it is possible to have an overview of the macrostructure of the samples. From Figure 2.7, it is possible to observe fibers with different sizes and the

agglomerations they formed. Using congo red dye helps for a better visualization of the fibers However, as mentioned above, we cannot see in detail the morphology and exact dimensions of the samples.

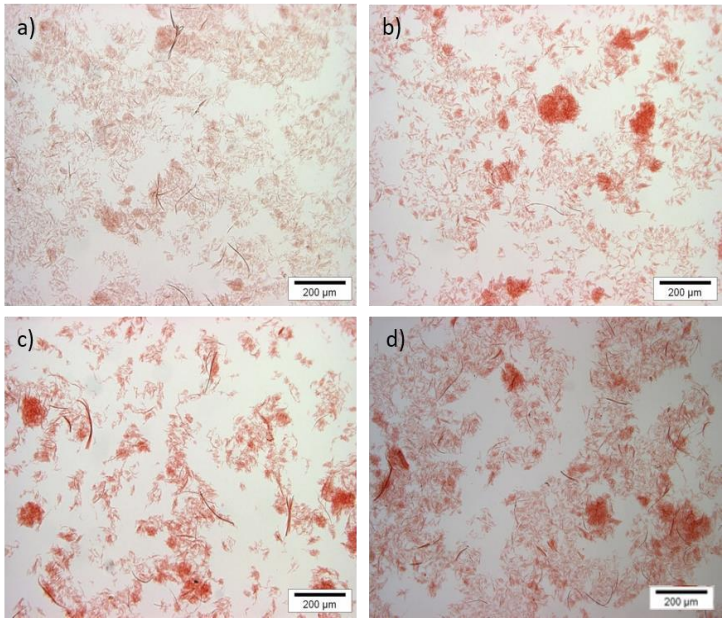

Figure 2.8. Optical microscopy of LCNF containing a) 0.6, b) 1.7, c) 4.7, and d) 10.2 % of lignin.

SEM images were obtained at a magnification of 5000X, allowing the visualization of the fibrillar structure of the samples (Figure 2.9). Could be suggested that the diameters of the fibrils are in the nano-scale size while the lengths are in the micrometer scale. However, to properly measure the dimensions of the fibers, higher magnifications are needed which were obtained by using atomic force microscopy (AFM).

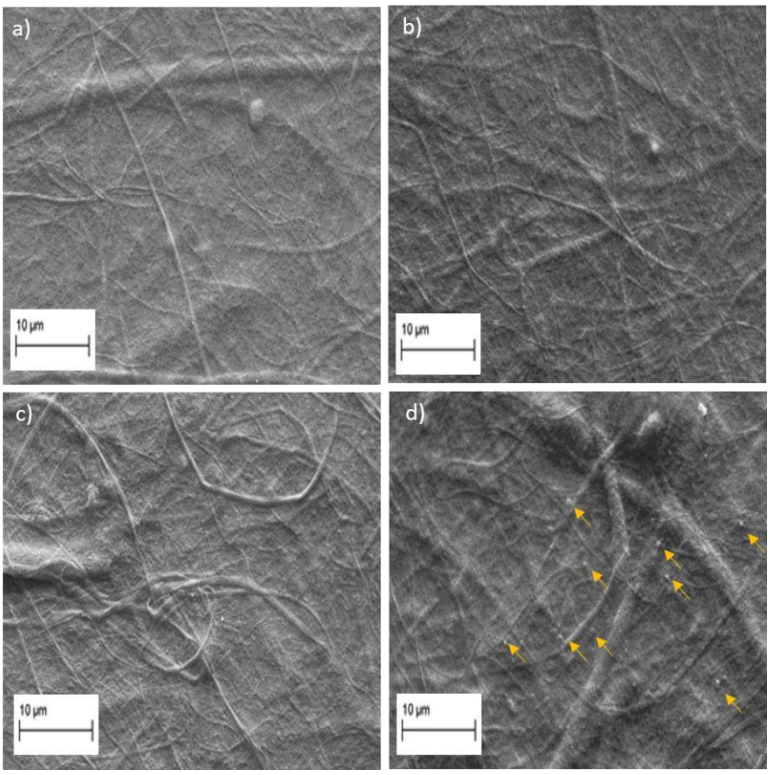

Figure 2.9. Scanning Electron Microscopies (SEM) of LCNF containing a) 0.6, b) 1.7, c) 4.7, and d) 10.2 % of lignin

SEM images for samples containing 10.2 % of lignin reveal the presence of spherical particles distributed along the surface. It is believed that such spheres correspond to lignin nanoparticles, which are released from the fibrillar structure due to the applied mechanical processes to obtain the LCNF.

AFM images were obtained in tapping mode and the analyzed amplitude images are presented in Figure 2.10. Using the AFM technique, the presence of globular-shape particles was proved, suggesting that those globular structures may correspond to lignin nanoparticles. Similar structures have been reported on the literature confirming their distribution over the fiber surfaces (Rojo et al. 2015; Bian et al. 2017a; Herrera et al. 2018). Our observations are consistent with

those reported in the literature (Rojo et al. 2015), the amount of these globular particles on the micrographs increases as the lignin content of the samples increases.

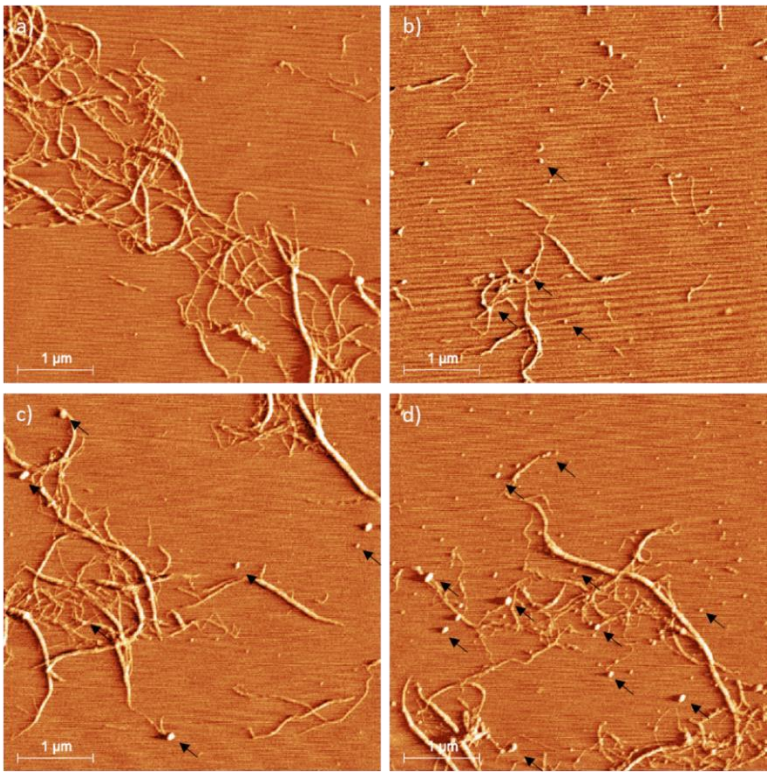

Figure 2.10. Atomic Force Microscopies (AFM) of LCNF containing a) 0.6, b) 1.7, c) 4.7, and d) 10.2 % of lignin

Although it was probed the presence of spherical nanoparticles, higher magnifications are necessary to confirmed where those particles are located, between the fibers, onto the fibers, or both. Besides, future analysis is required to confirm the chemical composition of these samples and to assure they are indeed lignin particles (i.e. nanoTA, XPS, and Tof-SIMS).

To analyze the diameter distributions of the fibrils based on the different lignin contents, AFM images were collected from five different zones of the coated surface (Figure 2.10).

Diameters from 100 fibrils from each sample were quantified using the J Image Software. As can be seen on Figure 2.11, the fibril diameters are not homogeneous, thus, the distribution of diameters were grouped in nine different ranges where the majority of the samples diameters are in a range from 0.0 to 0.09 μm.

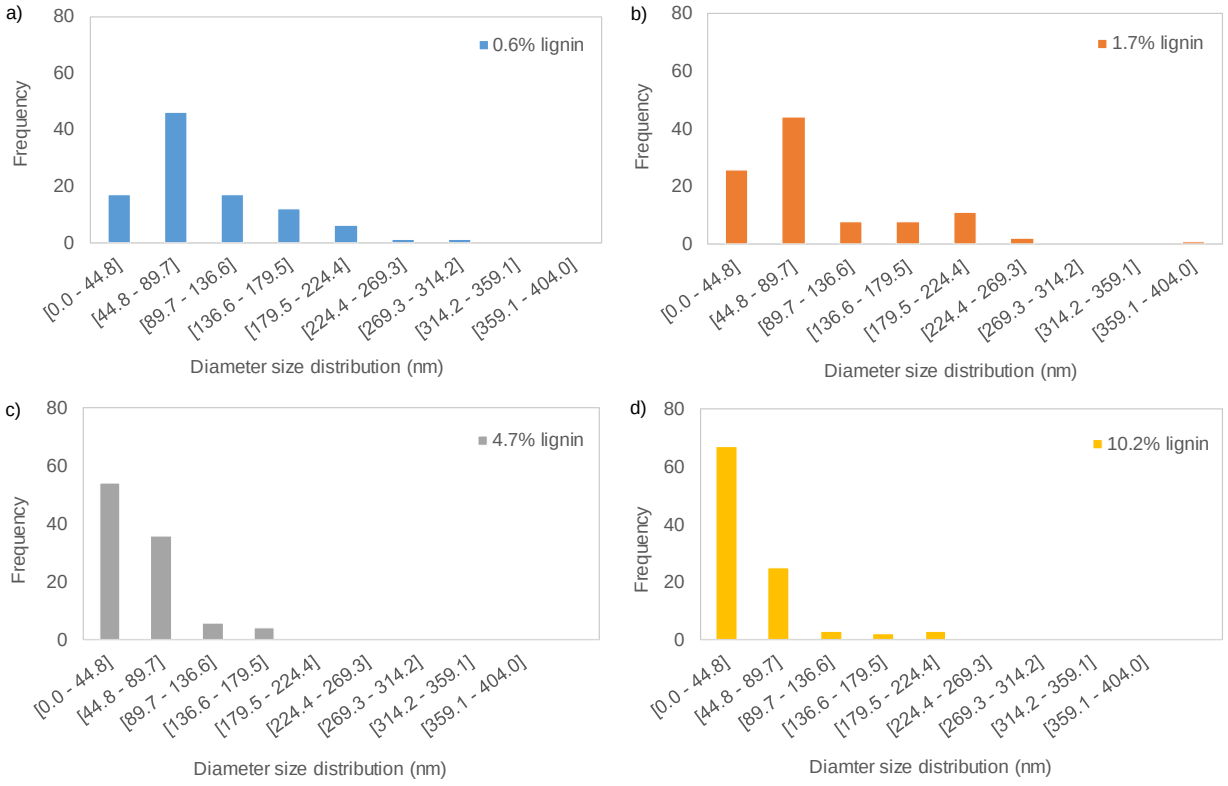

Figure 2.11. Diameters distribution for LCNF samples containing; a) 0.6, b) 1.7, c) 4.7, and d) 10.2% of lignin.

As the lignin content of the samples increase, fibrils diameters are smaller. For the range [0.0 – 0.045] μm which has the highest amount of fibrils, the mean fibrils diameter and standard deviations were 34.3 ± 8.7, 33.6 ± 9.2, 27.5 ± 10.2, and 20.2 ± 9.8 nm for samples containing 0.6, 1.7, 4.7, and 10.2 % of lignin, respectively. Rojo et al. (2015) proposed that due to the radical

scavenging ability of lignin which induce the stability of the radicals during the mechanical defibrillation (Solala 2011), as the amount of lignin on the LCNF increases, the possibility of attraction between the fibrils decrease, favoring the separation of the fibers. Consequently, smaller fibrils diameters are obtained at higher lignin contents. Our results suggest that the stabilization of free radicals promote the reduction of fibrils diameters together with the increase of hemicellulose content increase the repulsion among the fibrils. Consequently, a reduction of the crosslink and a better defibrillation of the samples could be expected.

2.4.3.7. Rheological measurements

The dynamic viscoelastic properties of LCNF samples were successfully assessed. Analyzing the flow curves (Figure 2.12) they follow a linear relation with the amount of lignin. At lower shear rates, the higher the lignin content, the higher the viscosity for all LCNF samples. By increasing the shear rate, particularly at values approximately of 4.22 s^{-1} the sample with 4.7 % lignin shows a disruption on the up-flow curves. For the down-flow curves, a disruption is also observed at 28 s^{-1} for the two samples with the highest lignin content which could be correlated to the lignin content present on each sample. As the shear rate increases, samples with 4.7 and 10.2 % lignin show similar viscosity values since their curves overlap, and a similar trend can be observed for the pair of samples with 0.6 and 1.7 % lignin.

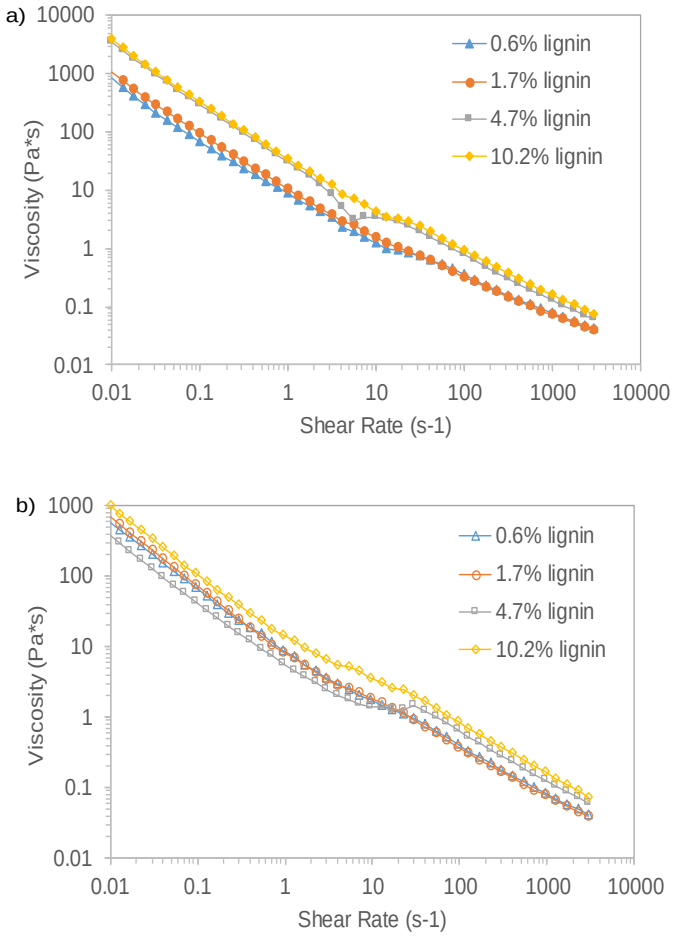

Figure 2.12. Steady state flow curves for LCNF a) UP curves, and b) DOWN curves.

Analyzing the up and down flow curves for each sample (Figure 2.13), the hysteresis of the curves can be clearly observed. For LCNF containing 0.6 and 1.7 % lignin (Figure 2.13.a and b), after the cycle was completed, the viscosity returned to its original value or very close to it. In the case of the samples containing 4.7 and 10.2 % lignin (Figure 2.13.c) and d), the viscosity decreased almost one order of magnitude. Such behavior can be explained by the fact that, at the beginning of the measurement, fibers are linked together by electrostatic interactions and H-bonds. While increasing the shear rate, fibers reorient themselves and steric forces start playing an

important role on the fibrillar structure since lignin is a three dimensional polymer with a branched structure. Thus, steric hindrance between the fibers breakdown the fibrillar network in an irreversible mode. In addition to this analysis, it was possible to assess the shear-thinning behavior reported in the literature for cellulose nanofibrils, where a decrease on the viscosity is accompanied by an increase in the shear rate (Herrick et al. 1983; Pääkko et al. 2007; Agoda-Tandjawa et al. 2010; Iotti et al. 2011; Karppinen et al. 2011; Tanaka et al. 2015).

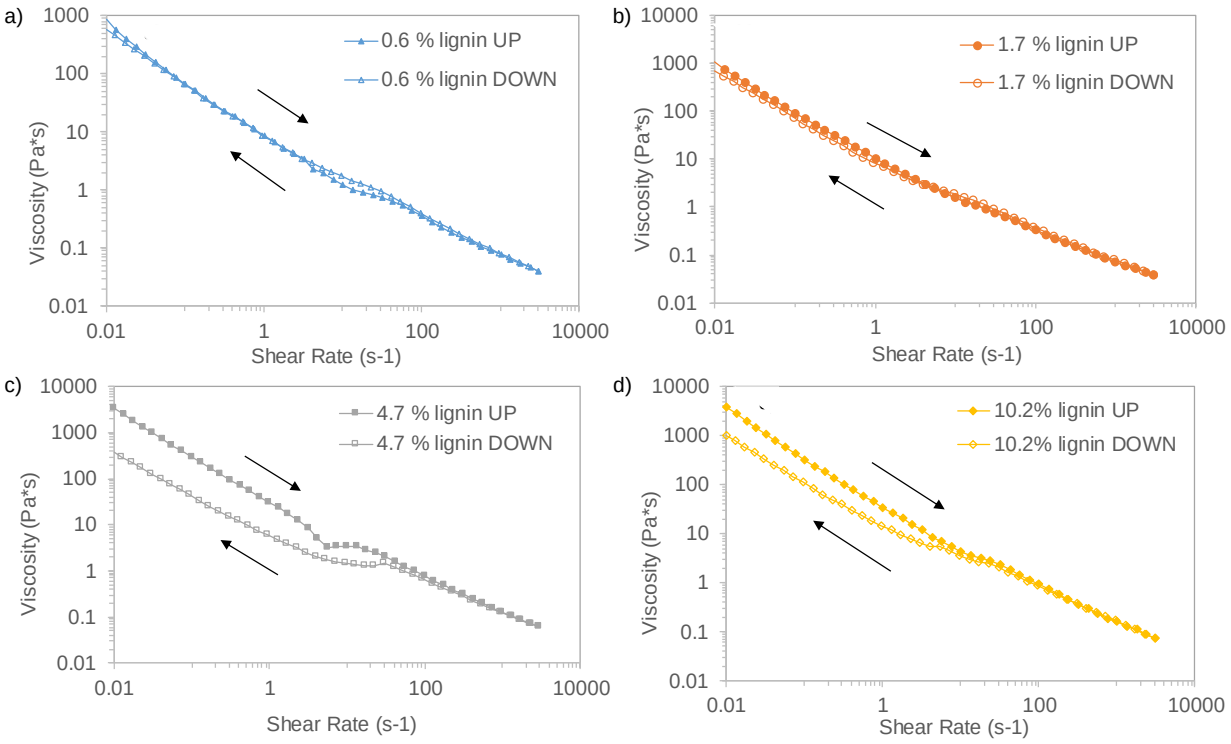

Figure 2.13. Up and down flow curves for L-CNF a) 0.6% lignin, b) 1.7% lignin, c) 4.7% lignin, and d) 10.2 % lignin.

Power-law parameters and regression values (R^2) were calculated for the fitted-UP curves, which are shown in Table 2.5. It has been reported in the literature that almost all non-Newtonian

fluids have a power index < 1 meaning they follow a shear-thinning behavior (Macosko 1994); which can be confirmed for all the samples containing lignin since they have power indexes < 0.3. All the R^2 values were very close to 1 indicating that fitting the data with the power-law model is a good approximation. Similar results were reported for bleached cellulose nanofibrils suspensions (Nazari et al. 2016).

Table 2.5. Power-law parameters and regression values (R^2) fitted to the data ($\eta = K\dot{\gamma}^{n-1}$) (Macosko 1994).

Sample (lignin content)	K ($Pa*s^n$)	n	R^2
0.6 %	11.511	0.267	0.9880
1.7 %	13.885	0.200	0.9909
4.7 %	37.463	0.145	0.9897
10.2 %	44.347	0.155	0.9937

Frequency sweeps curves are useful for studying the viscoelastic nature of the samples which is determined based on the magnitude of the storage moduli (G') compared to the loss moduli (G''). As can be seen on Figure 2.14 for all LCNF, G' is larger than G'' across the entire frequency range, which confirms a gel-like behavior of the samples. Although samples containing 0.6 % lignin show a higher G' and G'' than LCNF containing 1.7 % lignin, the variance could be not taken into account since the difference in lignin content is very small. Thus, it can be assumed that there is a linear relation between the lignin content and the values of G' and G''. Samples containing 10.2 % lignin had the highest G' and G'' values which is suggested to be due to the highest amount of lignin and hemicelluloses.

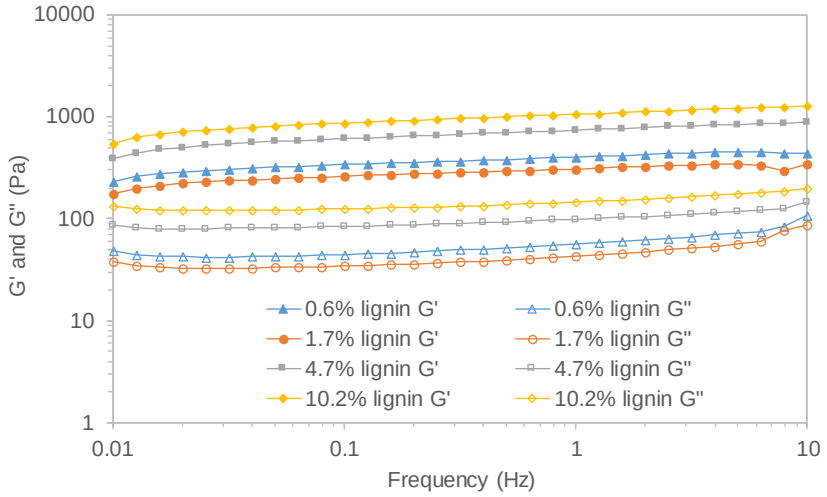

Figure 2.14. Oscillation curves for LCNF samples with an applied stress of 5 Pa. G' (bold), G'' (empty) for 0.6% lignin (▲,Δ), 1.7% lignin (●,○), 4.7% lignin (■, □), and 10.2% lignin (♦,◊).

No pre-shear was considered in these measurements. After 10 Hz, the inertial effects start affecting the acquisition of the data defining the range of measurement from 0.01 to 10 Hz.

Effect of pH

The importance of the effect of the pH on the rheological behavior of nanocellulose suspensions is related with the deprotonation of the carboxylic groups on the fibers surface which at pH larger than 4 are dissociated, increasing the repulsions between the fibrils and generating as a consequence, a reduction of the viscosity (Hubbe et al. 2017). Nevertheless, from Figure 2.15, the opposite behavior can be observed.

Flow curves of the sample containing 10.2 % of lignin were measured at pH 5 and 7, showing an increase in the viscosity as the pH increased. In the case of bleached microfibrillated cellulose, the opposite behavior has been reported by Pääkko et al. (2007), who observed the decrease of the viscosity with increasing pH values. On the other hand, Agoda-Tandjawa et al.

(2010) did not observe changes in the viscoelastic properties of cellulose suspensions when varying the pH.

In our studies, the increase of the viscosity when the pH increased could be explained due to the physical interactions within the fibrils structures which are smaller and can generate entanglements easily when a deformation is apply, and the steric repulsions due to the higher amount of lignin present on the samples. The presence of lignin may overcome the repulsive effect of the deprotonated carboxylic groups, reducing their effect.

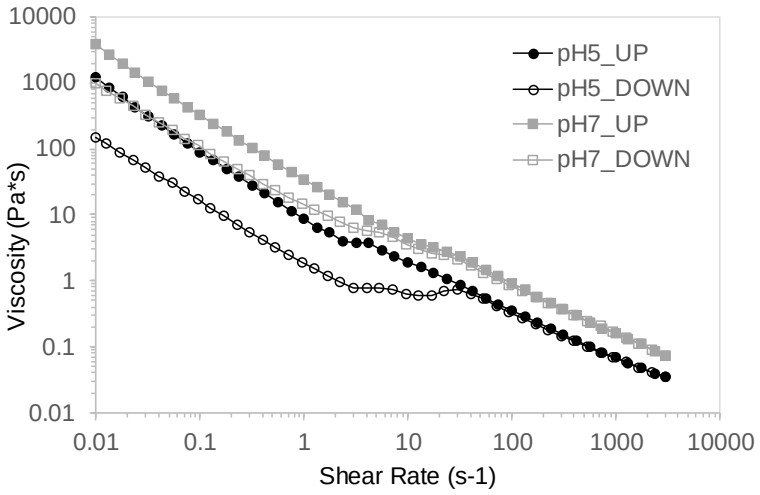

Figure 2.15. Rheological behavior of a LCNF containing 10.2 % at pH = 5 (● and ○), and pH = 7 (■ and □).

2.4.3.8. Surface contact angle measurements (SCA)

Surface Contact Angle (SCA) was expected to be affected by the chemical composition of the fibrils. Determination of the SCA was based on the analysis of the drop shape onto the surface. Eight different regions of each sample were measured. The angles between the drop and the

surfaces were measured every second during 30 sec. The average of the measurements and their standards deviations are presented on Table 2.6.

Table 2.6. SCA average results and standard deviations

Time (sec)	Sample (lignin content)			
	0.6 %	**1.7 %**	**4.7 %**	**10.2 %**
5	39.23±0.98	37.86±0.48	37.66±1.00	39.11±1.33
10	38.74±0.88	37.37±0.51	37.41±0.90	38.85±1.34
15	38.37±0.86	37.07±0.48	37.14±0.88	38.86±1.35
20	38.07±0.87	36.74±0.49	36.89±0.89	38.33±1.34
25	37.81±0.86	36.53±0.49	36.67±0.84	38.14±1.30
30	37.54±0.87	36.27±0.46	36.44±0.84	37.91±1.30

Analyzing the data from Table 2.6 is suggested that there are not significant differences between the samples. Future measurements will be performed using a selection of liquids to analyze the interactions of all the LCNF samples with liquids with different polarities. Besides, the roughness of the surface is a parameter that should be taken into consideration for further analysis.

2.5. Conclusions

In this work we have extensively analyzed how the chemical composition of LCNF samples, principally the amount of lignin and hemicelluloses, was related with their characteristics to further understand the rheological behavior of the samples.

Although lignin is considered as the binder of the cellulose fiber structure, holding together cellulose and hemicellulose, analyzing the diameters size distribution it was suggested that its

presence improves the defibrillation of the samples. Besides, using scanning electron microscopy and atomic force microscopy it was possible to confirm that after defibrillation process globular spheres, maybe lignin spheres, remained on the colloidal suspension mixed with the nanofibrils.

Rheological behavior was effectively assessed, showing an increase of the viscosity as the lignin content increased, and corroborating the shear thinning behavior of LCNF.

Although in consistent results were obtained by thermogravimetric analysis, the results suggested an incongruence of the results, making necessary further analysis.

After all the performed characterization techniques, it can be concluded that LCNF particles present very good properties and they should be considered for different applications due to their good properties and ease of production when compared with the fully bleached cellulose nanofibrils.

2.6. Future work

2.6.1. Use of LCNF as additive in drilling fluids

Drilling fluids play important functions during the drilling process such as, acting as lubricants between the tools and the formation, cleaning and stabilizing the well, and as filtration control (Aftab et al. 2017). Fluids are made-up by several components (Villada et al. 2017) being some of the commonly used additives, xanthan gum (Katzbauer 1998), polyanionic cellulose (Busch et al. 2018), starch (Dias et al. 2015), among others. Recently, the utilization of cellulose nanocrystals (CNC) and microfibrillar cellulose (MFC) from fully bleached cellulose pulp has been studied showing remarkable properties as additives in drilling fluids (Li et al. 2015a).

Due to the properties that lignin and hemicelluloses confer to LCNF when compared with BCNF, this renewable material has been proposed as an interesting alternative suitable as additive

in drilling fluids. Consequently, a study comparing the replacement of xanthan gum by using BCNF and LCNF was carried out (**Paper IV**) showing interesting performance. Besides, from an environmental and economical point of view, LCNF presents advantages with respect to BCNF.

2.6.2. Characterization techniques

Following with the research work presented on this thesis, we will continue with the study of lignin-containing cellulose nanofibrils. Some of the future measurements to be performed are; (1) rheological measurements varying pH, temperature, and consistency, (2) surface charge analysis by titration technique, (3) surface energy measurements using liquids with different polarities and considering roughness effect, (4) NanoTA and X-ray photoelectron spectroscopy (XPS) to gain a precise knowledge of the real location of lignin on the LCNF, and (5) electron paramagnetic resonance spectroscopy (EPR) analysis to study the scavenging lignin effect based on the stabilization of free radicals during the mechanical process.

References

Abbati de Assis C, Iglesias MC, Bilodeau M, et al (2017) Cellulose micro- and nanofi brils (CMNF) manufacturing - financial and risk assessment. Biofuels, Bioprod Biorefining 12:251–264. doi: 10.1002/bbb.1835

Aftab A, Ismail AR, Ibupoto ZH, et al (2017) Nanoparticles based drilling muds a solution to drill elevated temperature wells: A review. Renew Sustain Energy Rev 76:1301–1313. doi: 10.1016/j.rser.2017.03.050

Ago M, Ferrer A, Rojas OJ (2016) Starch-Based Biofoams Reinforced with Lignocellulose Nanofibrils from Residual Palm Empty Fruit Bunches: Water Sorption and Mechanical Strength. ACS Sustain Chem Eng 4:5546–5552. doi: 10.1021/acssuschemeng.6b01279

Agoda-Tandjawa G, Durand S, Berot S, et al (2010) Rheological characterization of microfibrillated cellulose suspensions after freezing. Carbohydr Polym 80:677–686. doi: 10.1016/j.carbpol.2009.11.045

Ballner D, Herzele S, Keckes J, et al (2016) Lignocellulose nanofiber-reinforced polystyrene produced from composite microspheres obtained in suspension polymerization shows superior mechanical performance. ACS Appl Mater interfaces 8:13520–13525. doi: 10.1021/acsami.6b01992

Belbekhouche S, Bras J, Siqueira G, et al (2011) Water sorption behavior and gas barrier properties of cellulose whiskers and microfibrils films. Carbohyd Polym 83:1740–1748. doi: 10.1016/j.carbpol.2010.10.036

Benhamou K, Dufresne A, Magnin A, et al (2014) Control of size and viscoelastic properties of nanofibrillated cellulose from palm tree by varying the TEMPO-mediated oxidation time. Carbohydr Polym 99:74–83. doi: 10.1016/j.carbpol.2013.08.032

Berthold F, Gustafsson K, Sjöholm E, et al (2001) An improved method for the determination of softwood kraft pulp molecular mass distribution. In: 11th International symposium on Wood and Pulping Chemistry. Nice, France, p Vol. I, 363-366

Bian H, Chen L, Dai H, et al (2017a) Integrated production of lignin containing cellulose nanocrystals (LCNC) and nanofibrils (LCNF) using an easily recyclable di-carboxylic acid. Carbohydr Polym 167:167–176. doi: 10.1016/j.carbpol.2017.03.050

Bian H, Chen L, Gleisner R, et al (2017b) Producing wood-based nanomaterials by rapid fractionation of wood at 80 °C using a recyclable acid hydrotrope. Green Chem 19:3370–3379. doi: 10.1039/C7GC00669A

Brebu M, Vasile C (2010) Thermal degradation of lignin—a review. Cellul Chem Technol 44:353–363

Busch A, Myrseth V, Khatibi M, et al (2018) Rheological characterization of polyanionic cellulose solutions with application to drilling fluids and cuttings transport modeling. Appl Rheol 28:32832. doi: 10.3933/APPLRHEOL-28-25154

Chen L, Zhu JY, Baez C, et al (2016) Highly thermal-stable and functional cellulose nanocrystals and nanofibrils produced using fully recyclable organic acids. Green Chem 18:3835–3843. doi: 10.1039/C6GC00687F

Cunha AG, Mougel JB, Cathala B, et al (2014) Preparation of double pickering emulsions stabilized by chemically tailored nanocelluloses. Langmuir 30:9327–9335. doi: 10.1021/la5017577

Delgado-Aguilar M, González I, Tarrés Q, et al (2016) The key role of lignin in the production of low-cost lignocellulosic nanofibres for papermaking applications. Ind Crops Prod 86:295–300. doi: 10.1016/j.indcrop.2016.04.010

Dias FTG, Souza RR, Lucas EF (2015) Influence of modified starches composition on their performance as fluid loss additives in invert-emulsion drilling fluids. Fuel 140:711–716. doi: 10.1016/j.fuel.2014.09.074

Dimic-Misic K, Gane PAC, Paltakari J (2013) Micro and nanofibrillated cellulose as a rheology modifier additive in CMC-containing pigment-coating formulations. Ind Eng Chem Res 52:16066–16083. doi: 10.1021/ie4028878

Diop CIK, Tajvidi M, Bilodeau MA, et al (2017) Isolation of lignocellulose nanofibrils (LCNF) and application as adhesive replacement in wood composites: example of fiberboard. Cellulose 24:3037–3050. doi: 10.1007/s10570-017-1320-z

Espinosa E, Tarrés Q, Delgado-Aguilar M, et al (2016) Suitability of wheat straw semichemical pulp for the fabrication of lignocellulosic nanofibres and their application to papermaking slurries. Cellulose 23:837–852. doi: 10.1007/s10570-015-0807-8

Ferrer A, Hoeger IC, Lu X, et al (2016) Reinforcement of polypropylene with lignocellulose nanofibrils and compatibilization with biobased polymers. J Appl Polym Sci 133:43584–43864. doi: 10.1002/APP.43854

Ferrer A, Quintana E, Filpponen I, et al (2012) Effect of residual lignin and heteropolysaccharides in nanofibrillar cellulose and nanopaper from wood fibers. Cellulose 19:2179–2193. doi: 10.1007/s10570-012-9788-z

Guan Gong (2014) Rheological properties of nanocellulose material. In: Kristiina Oksman, Aji P Mathew, Pia Qvintus, et al. (eds) Handbook of green material. World Scientific, Singapore, p vi: 139-157

Hage R El, Brosse N, Chrusciel L, et al (2009) Characterization of milled wood lignin and ethanol organosolv lignin from miscanthus. Polym Degrad Stab 94:1632–1638. doi:

10.1016/j.polymdegradstab.2009.07.007

Henriksson M, Henriksson G, Berglund LA, et al (2007) An environmentally friendly method for enzyme-assisted preparation of microfibrillated cellulose (MFC) nanofibers. Eur Polym J 43:3434–3441. doi: 10.1016/j.eurpolymj.2007.05.038

Herrera M, Thitiwutthisakul K, Yang X, et al (2018) Preparation and evaluation of high-lignin content cellulose nanofibrils from eucalyptus pulp. Cellulose 25:3121–3133. doi: 10.1007/s10570-018-1764-9

Herrick FW, Casebier RL, Hamilton KJ, et al (1983) Microfibrillated cellulose: morphology and accessibility. J Appl Polym Sci Appl Polym Symp 37:797–813

Herzele S, Veigel S, Liebner F, et al (2016) Reinforcement of polycaprolactone with microfibrillated lignocellulose. Ind Crops Prod 93:302–308. doi: 10.1016/j.indcrop.2015.12.051

Horseman T, Tajvidi M, Diop CIK, et al (2017) Preparation and property assessment of neat lignocellulose nanofibrils (LCNF) and their composite films. Cellulose 24:2455–2468. doi: 10.1007/s10570-017-1266-1

Huang Y, Wang Z, Wang L, et al (2016) Analysis of lignin aromatic structure in wood fractions based on IR spectroscopy. J Wood Chem Technol 36:377–382. doi: 10.1080/02773813.2016.1179325

Hubbe M, Rojas OJ, Lucia L, et al (2008) Cellulosic Nanocomposites: a Review. BioResources 3:929–980. doi: 10.15376/biores.3.3.929-980

Hubbe MA, Tayeb P, Joyce M, et al (2017) Rheology of nanocellulose-rich aqueous suspensions: A review. BioResources 12:9556–9661. doi: 10.15376/biores.12.4.Hubbe

Hult EL, Iotti M, Lenes M (2010) Efficient approach to high barrier packaging using microfibrillar

cellulose and shellac. Cellulose 17:575–586. doi: 10.1007/s10570-010-9408-8

Iotti M, Gregersen ØW, Moe S, et al (2011) Rheological studies of microfibrillar cellulose water dispersions. J Polym Environ 19:137–145. doi: 10.1007/s10924-010-0248-2

Isogai A, Saito T, Fukuzumi H (2011) TEMPO-oxidized cellulose nanofibers. Nanoscale 3:71–85. doi: 10.1039/C0NR00583E

Jonoobi M, Oladi R, Davoudpour Y, et al (2015) Different preparation methods and properties of nanostructured cellulose from various natural resources and residues: a review. Cellulose 22:935–969. doi: 10.1007/s10570-015-0551-0

Kajanto I, Kosonen M (2012) The potential use of micro-and nanofibrillated cellulose as a reinforcing element in paper. J Sci Technol For Prod Process 2:42–48

Karppinen A, Vesterinen AH, Saarinen T, et al (2011) Effect of cationic polymethacrylates on the rheology and flocculation of microfibrillated cellulose. Cellulose 18:1381–1390. doi: 10.1007/s10570-011-9597-9

Katzbauer B (1998) Properties and applications of xanthan gum. Polym Degrad Stab 59:81–84. doi: 10.1016/S0141-3910(97)00180-8

Kimura K, Kikuchi S, Yamasaki S (1999) Accurate root length measurement by image analysis. Plant Soil 216:117–127. doi: 10.1016/j.agwat.2007.03.002

Klemm D, Kramer F, Moritz S, et al (2011) Nanocelluloses: A new family of nature-based materials. Angew Chemie - Int Ed 50:5438–5466. doi: 10.1002/anie.201001273

Lahtinen P, Liukkonen S, Pere J, et al (2014) A Comparative study of fibrillated fibers from different mechanical and chemical pulps. BioResources 9:2115–2127. doi: 10.15376/biores.9.2.2115-2127

Larkin PJ (2011) Unknown IR and raman spectra. In: IR and Raman Spectroscopy - Principles and

Spectral Interpretation. Elsevier, United States, pp 177–212

Lee KY, Aitomäki Y, Berglund LA, et al (2014) On the use of nanocellulose as reinforcement in polymer matrix composites. Compos Sci Technol 105:15–27. doi: 10.1016/j.compscitech.2014.08.032

Lee SYSS, Mohan DJ, Kang IIA, et al (2009) Nanocellulose reinforced PVA composite films: effects of acid treatment and filler loading. Fibers Polym 10:77–82. doi: 10.1007/s12221-009-0077-x

Li MC, Wu Q, Song K, et al (2015a) Cellulose nanoparticles as modifiers for rheology and fluid loss in bentonite water-based fluids. ACS Appl Mater Interfaces 7:5009–5016. doi: 10.1021/acsami.5b00498

Li MC, Wu Q, Song K, et al (2015b) Cellulose Nanoparticles: Structure-Morphology-Rheology Relationships. ACS Sustain Chem Eng 3:821–832. doi: 10.1021/acssuschemeng.5b00144

Liu C, Du H, Dong L, et al (2017a) Properties of nanocelluloses and their application as rheology modifier in paper coating. Ind Eng Chem Res 56:8264–8273. doi: 10.1021/acs.iecr.7b01804

Liu Y, Gordeyeva K, Bergström L (2017b) Steady-shear and viscoelastic properties of cellulose nanofibril-nanoclay dispersions. Cellulose 24:1815–1824. doi: 10.1007/s10570-017-1211-3

Macosko CW (1994) Rheology: Principle, measurements, and applications. WILEY-VCH Verlag GmbH &Co., Canada

Missoum K, Martoïa F, Belgacem MN, et al (2013) Effect of chemically modified nanofibrillated cellulose addition on the properties of fiber-based materials. Ind Crops Prod 48:98–105. doi: 10.1016/j.indcrop.2013.04.013

Murwanashyaka JN, Pakdel H, Roy C (2001) Step-wise and one-step vacuum pyrolysis of birch-derived biomass to monitor the evolution of phenols. J Anal Appl Pyrolysis 60:219–231. doi:

10.1016/S0165-2370(00)00206-0

Naderi A, Lindström T, Sundström J (2014) Carboxymethylated nanofibrillated cellulose: Rheological studies. Cellulose 21:1561–1571. doi: 10.1007/s10570-014-0192-8

Nair SS, Kuo P-Y, Chen H, et al (2017) Investigating the effect of lignin on the mechanical, thermal, and barrier properties of cellulose nanofibril reinforced epoxy composite. Ind Crops Prod 100:208–217. doi: 10.1016/j.indcrop.2017.02.032

Nazari B, Kumar V, Bousfield DW, et al (2016) Rheology of cellulose nanofibers suspensions: boundary driven flow. J Rheol (N Y N Y) 60:1151–1159. doi: 10.1122/1.4960336

Okita Y, Saito T, Isogai A (2010) Entire surface oxidation of various cellulose microfibrils by TEMPO-mediated oxidation. Biomacromolecules. doi: 10.1021/bm100214b

Pääkko M, Ankerfors M, Kosonen H, et al (2007) Enzymatic hydrolysis combined with mechanical shearing and high-pressure homogenization for nanoscale cellulose fibrils and strong gels. Biomacromolecules 8:1934–1941. doi: 10.1021/bm061215p

Postek MT, Vladár A, Dagata J, et al (2011) Development of the metrology and imaging of cellulose nanocrystals. Meas Sci Technol 22:024005–024015. doi: 10.1088/0957-0233/22/2/024005

Potthast A, Radosta S, Saake B, et al (2015) Comparison testing of methods for gel permeation chromatography of cellulose: coming closer to a standard protocol. Cellulose 22:1591–1613. doi: 10.1007/s10570-015-0586-2

Rezayati Charani P, Dehghani-Firouzabadi M, Afra E, et al (2013) Rheological characterization of high concentrated MFC gel from kenaf unbleached pulp. Cellulose 20:727–740. doi: 10.1007/s10570-013-9862-1

Rojo E, Peresin MS, Sampson WW, et al (2015) Comprehensive elucidation of the effect of

residual lignin on the physical, barrier, mechanical and surface properties of nanocellulose films. Green Chem 17:1853–1866. doi: 10.1039/C4GC02398F

Saito T, Kimura S, Nishiyama Y, et al (2007) Cellulose nanofibers prepared by TEMPO-mediated oxidation of native cellulose. Biomacromolecules 8:2485–2491. doi: 10.1021/bm0703970

Segal L, Creely JJ, Martin AE, et al (1959) An Empirical Method for Estimating the Degree of Crystallinity of Native Cellulose Using the X-Ray Diffractometer. Text Res J 29:786–794. doi: 10.1177/004051755902901003

Sevastyanova O, Helander M, Chowdhury S, et al (2014) Tailoring the molecular and thermo-mechanical properties of kraft lignin by ultrafiltration. J Appl Polym Sci 131:40799–40810. doi: 10.1002/APP.40799

Siró I, Plackett D (2010) Microfibrillated cellulose and new nanocomposite materials: A review. Cellulose 17:459–494. doi: 10.1007/s10570-010-9405-y

Solala I (2011) Mechanochemical reactions in lignocelluloseic materials. Dissertation, Aalto Universty

Spence KL, Venditti RA, Rojas OJ, et al (2010) The effect of chemical composition on microfibrillar cellulose films from wood pulps: Water interactions and physical properties for packaging applications. Cellulose 17:835–848. doi: 10.1007/s10570-010-9424-8

Sun H, Wang X, Zhang L (2014) Preparation and characterization of poly(lactic acid) nanocomposites reinforced with Lignin-containing cellulose nanofibrils. Polym 38:464–470. doi: 10.7317/pk.2014.38.4.464

Taipale T, Österberg M, Nykänen A, et al (2010) Effect of microfibrillated cellulose and fines on the drainage of kraft pulp suspension and paper strength. Cellulose 17:1005–1020. doi: 10.1007/s10570-010-9431-9

Tanaka R, Saito T, Hondo H, et al (2015) Influence of flexibility and dimensions of nanocelluloses on the flow properties of their aqueous dispersions. Biomacromolecules 16:2127–2131. doi: 10.1021/acs.biomac.5b00539

Tong WY, bin Abdullah AYK, binti Rozman NAS, et al (2018) Antimicrobial wound dressing film utilizing cellulose nanocrystal as drug delivery system for curcumin. Cellulose 25:631–638. doi: 10.1007/s10570-017-1562-9

Turbak A, Snyder F, Sandberg K (1983) Microfibrillated cellulose. US Pat 4,374,702 11:1–11. doi: 10.1145/634067.634234.

Vallejos ME, Felissia FE, Area MC, et al (2016) Nanofibrillated cellulose (CNF) from eucalyptus sawdust as a dry strength agent of unrefined eucalyptus handsheets. Carbohydr Polym 139:99–105. doi: 10.1016/j.carbpol.2015.12.004

Villada Y, Gallardo F, Erdmann E, et al (2017) Functional characterization on colloidal suspensions containing xanthan gum (XGD) and polyanionic cellulose (PAC) used in drilling fluids for a shale formation. Appl Clay Sci 149:59–66. doi: 10.1016/j.clay.2017.08.020

Visanko M, Sirviö JA, Piltonen P, et al (2017) Castor oil-based biopolyurethane reinforced with wood microfibers derived from mechanical pulp. Cellulose 24:2531–2543. doi: 10.1007/s10570-017-1286-x

Wågberg L, Winter L, Ödberg L, et al (1987) On the charge stoichiometry upon adsorption of a cationic polyelectrolyte on cellulosic materials. Colloids and Surfaces 27:163–173. doi: 10.1016/0166-6622(87)80335-9

Wang C, Kelley SS, Venditti RA (2016) Lignin-based thermoplastic materials. ChemSusChem 9:770–783. doi: 10.1002/cssc.201501531

Wang X, Sun H, Bai H, et al (2014) Thermal, mechanical, and degradation properties of

nanocomposites prepared using lignin-cellulose nanofibers and poly(Lactic Acid). BioResources 9:3211–3224

Xu X, Liu F, Jiang L, et al (2013) Cellulose nanocrystals vs. Cellulose nanofibrils: A comparative study on their microstructures and effects as polymer reinforcing agents. ACS Appl Mater Interfaces 5:2999–3009. doi: 10.1021/am302624t

Yang H, Yan R, Chen H, et al (2007) Characteristics of hemicellulose, cellulose and lignin pyrolysis. Fuel 86:1781–1788. doi: 10.1016/j.fuel.2006.12.013

Zimmermann T, Bordeanu N, Strub E (2010) Properties of nanofibrillated cellulose from different raw materials and its reinforcement potential. Carbohydr Polym 79:1086–1093. doi: 10.1016/j.carbpol.2009.10.045